AGU ADVANCING EARTH AND SPACE SCIENCE

Reviews of Geophysics

REVIEW ARTICLE
10.1029/2020RG000727

On the Cause of the Mid-Pleistocene Transition

C. J. Berends[1], P. Köhler[2], L. J. Lourens[3], and R. S. W. van de Wal[1,4]

[1]Institute for Marine and Atmospheric Research Utrecht, Utrecht University, Utrecht, The Netherlands, [2]Alfred-Wegener-Institut, Helmholtz-Zentrum für Polar-und Meeresforschung, Bremerhaven, Germany, [3]Department of Earth Sciences, Faculty of Geosciences, Utrecht University, Utrecht, The Netherlands, [4]Department of Physical Geography, Faculty of Geosciences, Utrecht University, Utrecht, The Netherlands

Key Points:

- Different physical mechanisms have been proposed to explain the Mid-Pleistocene Transition; all are plausible, none are certain
- Evidence of a Pleistocene cooling trend (required for many mechanisms to act) remains inconclusive
- More systematic model studies could help fill in the gaps in the current knowledge

Correspondence to:
C. J. Berends,
c.j.berends@uu.nl

Citation:
Berends, C. J., Köhler, P., Lourens, L. J., & van de Wal, R. S. W. (2021). On the cause of the mid-Pleistocene transition. *Reviews of Geophysics*, *59*, e2020RG000727. https://doi.org/10.1029/2020RG000727

Received 17 NOV 2020
Accepted 16 MAY 2021

Abstract The Mid-Pleistocene Transition (MPT), where the Pleistocene glacial cycles changed from 41 to ~100 kyr periodicity, is one of the most intriguing unsolved issues in the field of paleoclimatology. Over the course of over four decades of research, several different physical mechanisms have been proposed to explain the MPT, involving non-linear feedbacks between ice sheets and the global climate, the solid Earth, ocean circulation, and the carbon cycle. Here, we review these different mechanisms, comparing how each of them relates to the others, and to the currently available observational evidence. Based on this discussion, we identify the most important gaps in our current understanding of the MPT. We discuss how new model experiments, which focus on the quantitative differences between the different physical mechanisms, could help fill these gaps. The results of those experiments could help interpret available proxy evidence, as well as new evidence that is expected to become available.

Plain Language Summary For the past 1.2 million years, during the Late Pleistocene, the Earth has gone through glacial cycles ("ice ages") of ~120,000 years in duration. Before that, during the Early Pleistocene, glacial cycles lasted only ~41,000 years. The cause of this change in duration (called the "Mid-Pleistocene Transition", or MPT) is not clear. We review the different explanations for the MPT that have been proposed by different researchers over the past few decades, comparing them to each other and to the available evidence.

1. Introduction

Uncertainties in long-term projections of sea-level rise beyond the 21st century are dominated by the rate at which the Greenland and Antarctic ice sheets will melt in a warming climate (Oppenheimer et al., 2019). Since the response of these ice sheets to any change in climate occurs extremely slowly on the human time scale, observational evidence of ice-sheet retreat cannot sufficiently reduce these uncertainties. Instead, the research within paleoclimatology and paleoglaciology must help answer the question of how the ice sheets will evolve in a changing climate on long time scales. Scientists study the Pleistocene glacial cycles because they show dramatic changes in both global climate and ice-sheet size, as reflected in the landscape and in various different proxy archives. Although this research has been going on for almost two centuries, their potential for improving our understanding of the Earth's climate system in the context of anthropogenic climate change has made this field more relevant now than ever before.

The hypothesis that the Pleistocene glacial cycles were caused by small, periodic changes in the shape of Earth's orbit around the Sun, the result of gravitational perturbation by the Moon and the other planets in the solar system, was first proposed by Serbian scientist Milutin Milankovic (1941). Although the Scottish scientist James Croll proposed a very similar theory as early as 1875 (Fleming, 2006), he proposed a link to precession rather than to obliquity and/or eccentricity. The resulting prediction of 20 kyr glacial cyclicity led to his theory being rejected, and subsequently ignored for almost a century, by the scientific community. A revival occurred when Hays et al. (1976) published their isotopic analysis of a deep-sea sediment core, spanning over 400,000 years and clearly showing four distinct glacial cycles, introducing many new questions. Although spectral analysis of the isotopic signal indicated minor peaks at the precession (19/23 kyr) and obliquity (41 kyr) periodicities, the dominant peak occurred at ~100 kyr. This seemed to correspond to one of the eccentricity terms, which however provides only a small contribution to insolation changes. Later that year, Shackleton and Opdyke (1976) published results from another core, dating back well over two million years. Their findings complicated matters even further: Although their core displayed the same

apparent 100 kyr cyclicity in the Late Pleistocene, roughly 1.2 Myr ago to the present day, the Early Pleistocene (2.6–1.2 Myr ago) showed mostly consistent 41 kyr cycles, with an amplitude that was significantly smaller. After this shift in glacial periodicity was confirmed by the more detailed statistical and spectral analysis of the core data by Pisias and Moore (1981), it has become known as the Mid-Pleistocene Transition (MPT). To complicate matters further, later analyses found that interglacials during the Late Pleistocene do not actually appear every 100 kyr, but instead seemed to evolve toward integer multiples of the 41 kyr obliquity cycle (Huybers et al., 2007; Köhler & van de Wal, 2020; Past Interglacials Working Group of PAGES, 2016; Tzedakis et al., 2017).

These findings gave rise to two important questions:

(1) How can ~100 kyr glacial cycles occur in a world forced by insolation changes with only a very small 100 kyr term and much larger term for 20 and 40 kyr terms?
(2) Why did these ~100 kyr cycles only appear after the MPT, despite no obvious change in solar forcing around that time?

Answering these two questions has been an important goal in the fields of both paleoclimatology and paleoglaciology, as virtually all suggested mechanisms to explain the MPT could have some impact on projections of future ice-sheet evolution. As long as models cannot accurately reproduce the observed paleo-record (both the benthic oxygen isotope data from sediment cores, and the more recent data on CO_2 and other tracers from ice cores), they must lack some physical process(es). This means that tuning a model to reproduce, for example, observations of present-day ice-sheet geometry or bedrock uplift rates can result in compensating errors, which reduces the confidence in future projections of ice-sheet retreat.

In this review, we will discuss the different physical processes that have been proposed as explanations for both the ~100 kyr glacial periodicity of the Late Pleistocene, and for the change in periodicity that occurred during the MPT. We will begin by briefly reviewing the proxy evidence for the MPT (Section 2), as well as the Milankovic theory of orbital forcing of glacial cycles (Section 3), which demonstrates that orbital forcing alone cannot explain the transition. These two sections are deliberately kept brief, as comprehensive overviews of the proxy data are available in the literature; here we focus on the physical mechanisms behind the MPT. In Sections 4 and 5, we discuss the various physical mechanisms that have been proposed to explain the changing response to the unchanging orbital forcing, including different nonlinear feedbacks between ice sheets and the global climate, ocean circulation, and the carbon cycle. Many of these proposed mechanisms require the existence of a slow, steady cooling trend throughout the Pleistocene to explain the MPT. The evidence for the existence of such a cooling trend is discussed in Section 6, utilizing both proxy evidence and model studies. In Section 7, we summarize the current state of knowledge with respect to the mechanisms of the MPT, and describe possible new model experiments that could be of added value to guide both a physical understanding as well as providing guidance for further modeling and observational studies.

2. The MPT in Proxy Archives

The two most important sources of information for the Pleistocene glacial cycles are ice cores and sediment cores. Ice cores contain two important sources of paleoclimatic information. Their heavy water isotopes (δD, $\delta^{18}O$) can be used as a proxy for (local) paleotemperature (e.g., Dansgaard, 1964; Jouzel et al., 1997, 2007; Werner et al., 2018), and firn air trapped in bubbles and clathrates in the ice can be analyzed to determine the atmospheric concentrations of the three most important greenhouse gases (CO_2, CH_4, and N_2O). Currently, the ice core record extends back to 800 kyr (Bereiter et al., 2015; European Project for Ice Coring in Antarctica (EPICA) Community Members, 2004; Jouzel et al., 2007). The ongoing BEOIC (Beyond EPICA: Oldest Ice Core) project is expected to extend the Antarctic ice core records to 1,500 kyr (Sutter et al., 2019).

However, palaeoinformation based on marine records extends much further back in time. The $\delta^{18}O$ of fossil benthic foraminifera is governed by both the temperature of the ocean and the size of the world's ice sheets at the time the foraminifera lived, with higher values indicating both larger ice sheets and a colder climate. Following the publication of the iconic paper of Hays et al. (1976), many more cores have been drilled and analyzed. By aggregating records from different cores into stacks, uncertainties resulting from measurement

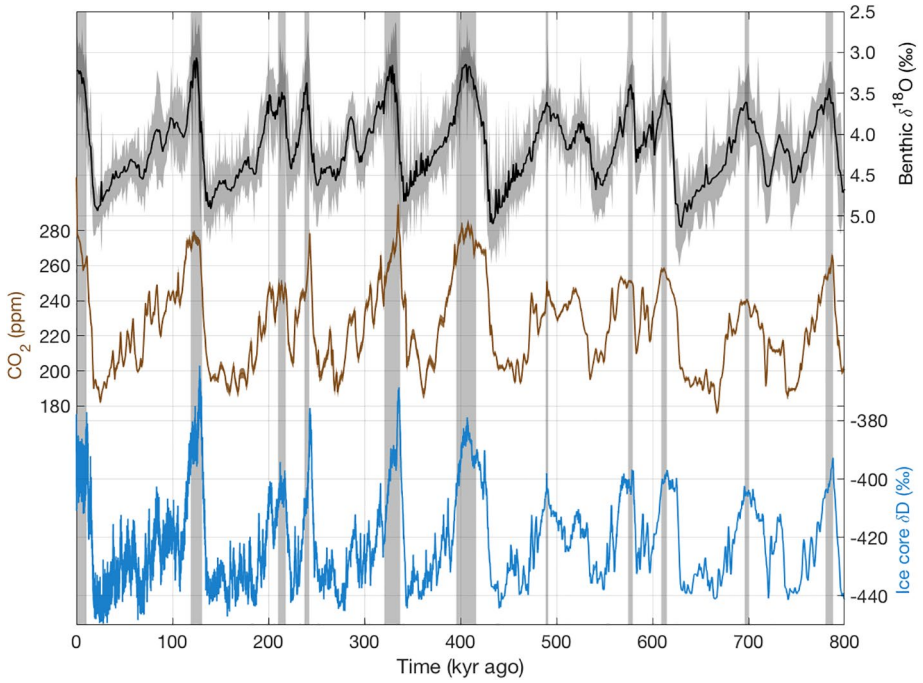

Figure 1. The benthic $\delta^{18}O$ stack by Ahn et al. (2017) (black, 95% confidence interval indicated by shaded area), the combined ice core CO_2 record by Bereiter et al. (2015) (brown), and the EPICA Dome C δD record by Jouzel et al. (2007) (blue, on the AICC2012 chronology; Veres et al., 2013; Bazin et al., 2013), for the past 800 kyr. Vertical shaded areas indicate the 11 interglacials as determined by the Past Interglacials Working Group of PAGES (2016).

errors, data gaps, age models, and other factors can be reduced. As new cores have become available, they have been combined into stacks of increasing size (Bassinot et al., 1994; Huybers & Wunsch, 2004; Imbrie et al., 1984; Karner et al., 2002; Lisiecki & Raymo, 2005; Pisias et al., 1984; Prell et al., 1986; Raymo et al., 1990; Williams et al., 1988). The most recent of these, created by Ahn et al. (2017), combines $\delta^{18}O$ data from 180 globally distributed cores, spanning the last 5 Myr.

Important paleorecords of the past 800 kyr are plotted in Figure 1: The benthic $\delta^{18}O$ stack by Ahn et al. (2017), the combined ice core CO_2 record by Bereiter et al. (2015), and the EPICA Dome C δD record by Jouzel et al. (2007) (on the AICC2012 chronology; Bazin et al., 2013; Veres et al., 2013). During the Late Pleistocene glacial cycles all three variables are roughly in phase (Jouzel et al., 2007), although during falling obliquity and the growth of land ice, CO_2 was partly decoupled from temperature and sea level (Barnola et al., 1987; Hasenclever et al., 2017; Köhler et al., 2018). Based on a careful analysis of multiple different proxy records, the Past Interglacials Working Group of PAGES (2016) identified 11 interglacials during this period, indicated in Figure 1, which nicely show that the temporal spacing between subsequent interglacials is in general larger than 41 kyr, but does not follow a unique periodicity.

The last 3.3 Myr of the benthic $\delta^{18}O$ stack by Ahn et al. (2017) is shown in Figure 2. The difference between the larger amplitude of the longer glacial cycles of the Late Pleistocene, and the smaller, shorter (41-kyr) cycles of the Early Pleistocene is clearly visible. The exact timing of the transition is not obvious; different studies have proposed both abrupt and gradual changes, occurring between 1,500 and 600 kyr ago (e.g., Clark et al., 2006; Dyez et al., 2018; Elderfield et al., 2012; Konijnendijk et al., 2015; Liu et al., 2008; McClymont et al., 2013; Nyman & Ditlevsen, 2019; Rutherford & D'Hondt, 2000; Schulz & Zeebe, 2006; Snyder, 2016). Clark et al. (2006) showed that the large spread in proposed timings can be explained, at least partly, by the variety of statistical tools that have been used to analyze the data (e.g., wavelet analysis, moving window Fourier transforms, change-point analysis) and the choice of timing criterion ($\delta^{18}O$ threshold, time between interglacials, peaks in wavelet spectrograms) as well as by the variety of data that are analyzed (e.g., different individual benthic $\delta^{18}O$ records from different locations, different stacks).

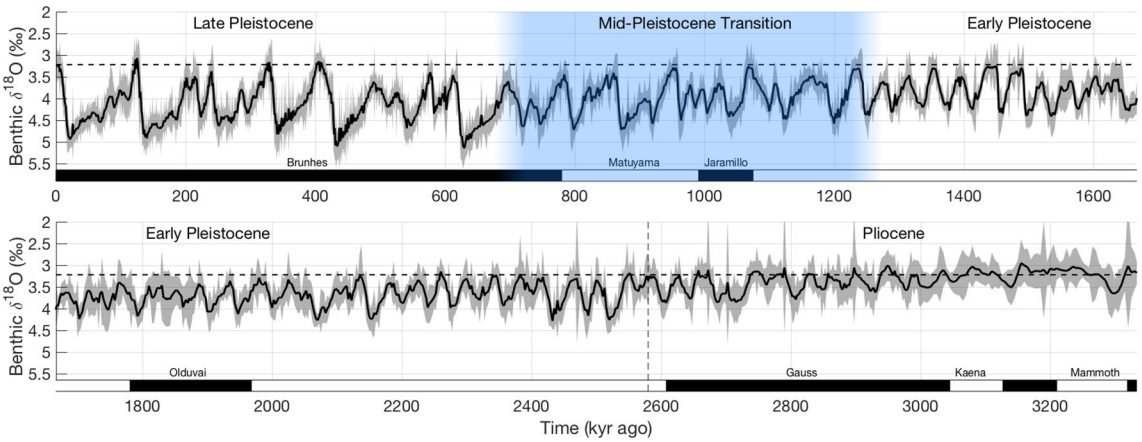

Figure 2. The last 3.3 Myr of the benthic $\delta^{18}O$ stack by Ahn et al. (2017) (uncertainty indicated by shaded area), plotted over magnetic reversal stages as indicated by the bars below the panels (Lisiecki & Raymo, 2005). The "transition phase" of the MPT is indicated by the blue shaded area.

The nature of the periodicity of the Late Pleistocene glacial cycles is also not obvious. Different studies have described them as regular 100 kyr cycles, arising from either internal oscillations, a strong amplification of weak eccentricity forcing, or a combination of both (Ganopolski & Calov, 2011; Gildor & Tziperman, 2001; Imbrie et al., 2011; Lisiecki, 2010), as alternating 82/100/123 kyr cycles, where several maxima in either obliquity, precession, or both, are "skipped" before the next one triggers a deglaciation (e.g., Huybers & Wunsch, 2005; Huybers, 2006, 2007; 2011; Köhler & van de Wal, 2020; Liu et al., 2008; Ridgwell et al., 1999; Tzedakis et al., 2017; Tziperman et al., 2006), and even as semi-random fluctuations with no true periodicity (Wunsch, 2003). Attempts to analyze the duration of the cycles are complicated by the fact that most proxy records are orbitally tuned, which leads to a circular problem when using those records for spectral analysis, or to investigate lead-lag relations with orbital forcing (Huybers & Wunsch, 2004). In order to discuss the role of insolation we briefly recap the orbital forcing in the next section.

Likewise, the characterization of the entire Early Pleistocene as having 41-kyr periodicity is a simplification, although most cycles were 41 kyr in duration. For example, around 2.5 Myr ago across MIS 100-96 subsequent deglaciations have been found to be first ~56 kyr, then ~28 kyr apart (Lourens et al., 2010). When defining interglacials by the absence of northern hemispheric land ice outside of Greenland, Köhler and van de Wal (2020) found that only 67% of the 41-kyr long obliquity cycle between 1.6 and 2.6 Myr ago led to the realization of a new interglacial, therefore, pointing to a partly irregular periodicity of climate for the Early Pleistocene.

3. Orbital Forcing

Milutin Milankovic (1941) proposed that the Earth's glacial cycles were a consequence of the small, periodic changes in the Earth's orbital and rotational parameters – specifically, the eccentricity of its orbit, the obliquity of its rotational axis, and the precession of both its rotational axis and the semi-major axis of its orbit. Milankovic showed that, while these astronomical cycles only had a very small effect on the total amount of energy reaching the Earth each year, the amount of sunlight received by one particular hemisphere during half a year changes considerably. Since glaciers and ice sheets are commonly understood to be more sensitive to changes in summer temperature than in winter, and since Earth's land mass (and therefore the space for glacier and ice sheets to grow) is mostly located in the Northern hemisphere, the astronomical cycles could have a strong effect on global ice volume. Orbital parameters of the Earth for the last 2 million years (Laskar et al., 2004), the resulting mean summer (June-July-August; JJA) insolation at 65°N, and the integrated summer insolation (ISI; Huybers, 2006) between 30° and 70°N are compiled in Figure 3.

As can be seen in the frequency spectra shown in the right-hand panels of Figure 3, the 65°N summer insolation is dominated by changes in precession, followed by the 41-kyr obliquity cycle. Huybers (2006) argues that, since precession affects not just the summer insolation but also the duration of summer (due to

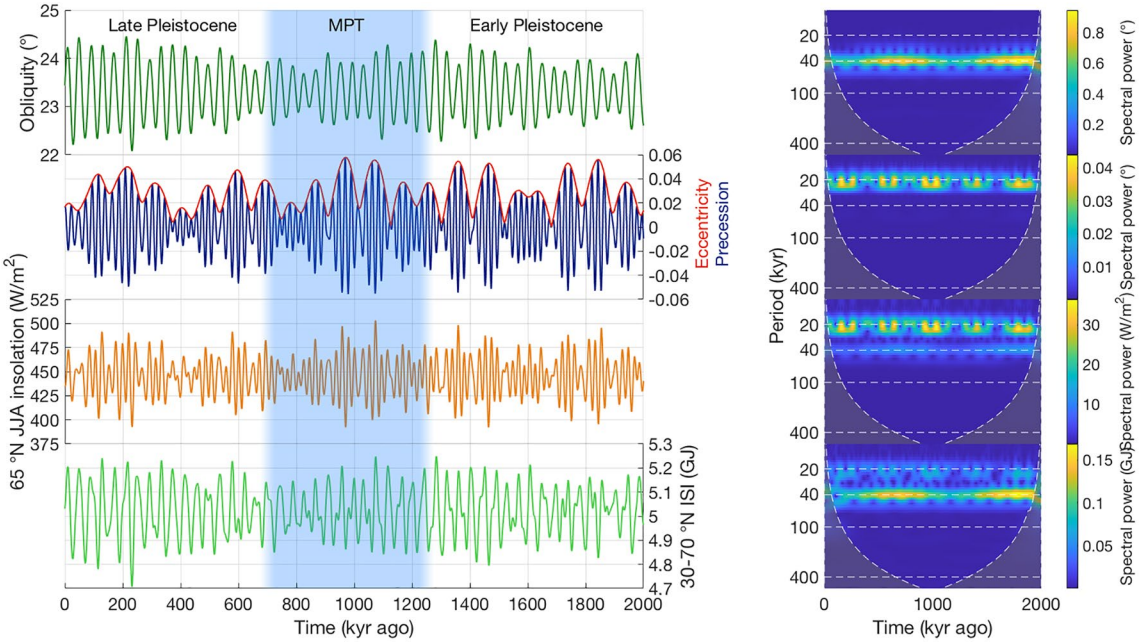

Figure 3. From top to bottom: Obliquity (green), eccentricity (red) and precession (blue) of the Earth, according to the solution by Laskar et al. (2004); the resulting summer (JJA, June-July-August) insolation at 65°N (orange), and the resulting integrated summer insolation (ISI) between 30° and 70°N (Huybers, 2006), all over the past 2 million years. The right-hand panels show the corresponding frequency scalograms from the wavelet transform.

the higher orbital velocity near perihelion), a more appropriate measure for the effect of orbital changes on glacier mass balance would be the ISI. In the ISI, the effects of precession on summer insolation and duration largely cancel out in the integral, leaving the 41-kyr obliquity cycle as the dominant term. The 100- and 400-kyr eccentricity cycles, which modulate the effects of precession, are not visible in the 65°N summer insolation, nor in the ISI. As can be seen directly from the frequency scalograms in Figure 3, as well as in more detailed statistical and spectral analyses (Clark et al., 2006; Lisiecki, 2010), the spectral nature of the solar forcing is statistically similar in both the Early and Late Pleistocene, so that there is no reason to believe that the change in the spectrum of reconstructed climate change over the MPT is solely driven by insolation.

4. Proposed Mechanisms Based on Ice-Sheet Feedbacks

This section discusses different feedback mechanisms that have been proposed as (contributing) causes of the MPT that mainly focus on ice sheets (ice-climate feedbacks, basal conditions, ice-dynamical instabilities, etc.). Mechanisms involving sea ice, ocean circulation, and the carbon cycle, will be discussed in Section 5.

4.1. A Framework of Ice-Sheet Stability Thresholds

Several different mechanisms that have been proposed to explain the so-called 100-kyr Late Pleistocene glacial cycles involve nonlinear feedback mechanisms between ice sheets and the global climate, the solid Earth, and other Earth system components (Abe-Ouchi et al., 2013; Bintanja & van de Wal, 2008; Clark & Pollard, 1998; Oerlemans, 1980; Pollard, 1983; Raymo, 1997). Here, we propose a framework, where the sensitivity of an ice sheet to changes in insolation and climate is separated into three size regimes, separated by two thresholds (Figure 4). In the "small" regime, the ice sheet is too small to survive an insolation maximum, leading to the nearly linear response of ice volume to the 41-kyr variations of ISI visible in reconstructions for the Early Pleistocene (Bintanja & van de Wal, 2008; Köhler & van de Wal, 2020). The "small" regime is separated from the "medium" regime by a threshold ice-sheet size. Above this threshold, certain positive feedbacks in the ice-sheet – climate system, such as the ice-albedo and elevation-temperature feedbacks, create enough self-sustained ice-sheet growth to allow the ice sheet to survive an insolation

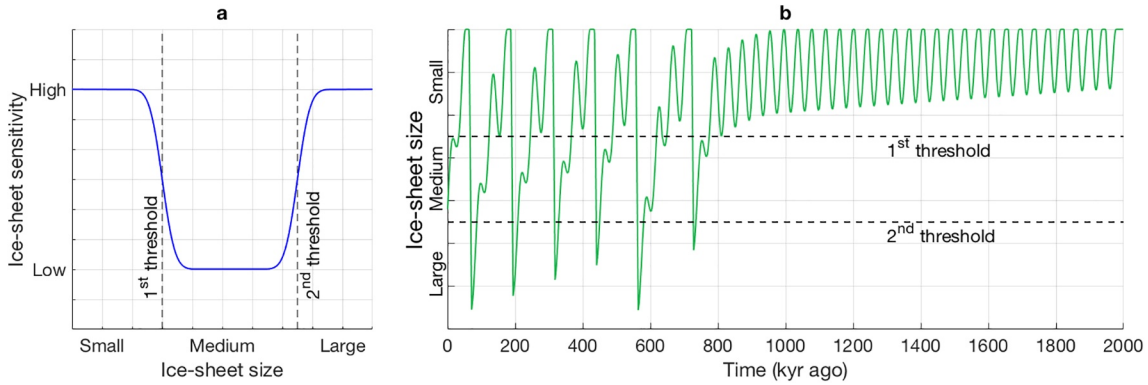

Figure 4. (a) The two-threshold framework. In the "small" regime, ice sheets are sensitive to changes in insolation, and react linearly. In the "medium" regime, self-sustained growth reduces melt during insolation maxima, resulting in a lower sensitivity. In the "large" regime, ice sheets become highly sensitive again, so that an insolation maximum can trigger a termination. (b) Ice-sheet size over time, from an extremely simple zero-dimensional model of this two-threshold system. The model is forced with a 41-kyr sinusoid insolation, plus a small linear cooling term.

maximum. The "medium" regime is separated from the "large" regime by a second threshold. Above this second threshold, different physical mechanisms, such as the bedrock-mass-balance feedback and calving, lead to the ice sheet becoming unstable or more vulnerable. An insolation maximum will then trigger a self-sustained retreat, leading to the rapid disintegration of the ice sheet. We will show that the majority of studies that propose different ice-dynamical processes as explanations for the MPT, fit within this two-threshold framework. All of these studies explain the MPT as the result of a slow, global cooling trend throughout the Pleistocene. Before the MPT, they suggest, global temperatures were warm enough that, during insolation minima, the ice sheet size never reached the first threshold. This implied that ice sheets were too small to survive an insolation maximum, consequently leading to a near-linear response of land ice volume to insolation, and a periodicity in ice-sheet size that is similar to that of the relevant incoming insolation (here 41 kyr). The MPT marks the point in time when temperatures became cold enough for the ice sheets to reach the size of the first threshold, thus surviving the next insolation maximum and continuing their growth through the next cycle of insolation or obliquity. This is repeated until the growing ice sheet crosses the second size threshold and becomes unstable. The next insolation maximum then triggers a deglaciation (or termination), moving the world to an interglacial state. The right-hand panel of Figure 4 shows how an extremely simple zero-dimensional model (see Appendix A) of such a two-threshold system, forced with a simple sinusoid insolation plus a linear cooling term, can reproduce the basic features of the MPT. Paillard (1998, 2001) showed that a similar three-regime model can, after some careful tuning, produce an ice volume history that closely matches the observed benthic $\delta^{18}O$ record in terms of the timing, duration, and relative magnitude of glacial cycles.

4.2. Positive Feedbacks for Ice-Sheet Growth

The existence of the lower threshold in ice sheet size in our framework has been linked to both the ice-albedo and elevation-temperature feedbacks. As an ice sheet advances, the bare soil and rock of the adjacent tundra become snow-covered for increasing parts of the year, until it gets covered by the ice sheet itself. Since the albedo of snow and ice is much higher than that of rock and soil, this locally reinforces the cooling that caused the initial ice-sheet advance, and also reduces the sensitivity of the local climate to changes in insolation. This effect has been known for a long time in the scientific literature (e.g., Budyko, 1969; Milankovic, 1941; Sellers, 1969), and several studies have been able to capture it in ice-sheet models without requiring full dynamic coupling to General Circulation Models (GCMs) (Abe-Ouchi et al., 2013; Berends et al., 2018). The elevation-temperature feedback (Weertman, 1961) is a basic atmospheric property based on adiabatic cooling; as a parcel of air moves up, the pressure drops, causing the air to both expand and cool. Since the mass balance of an ice sheet, and in particular the melt, strongly depends on temperature, this leads to a positive feedback, where ice-sheet growth leads to a surface cooling, reducing melt and enhancing the growth. Using a relatively simple one-dimensional (1-D) ice-sheet model, Clark and Pollard (1998) show how the elevation-temperature feedback can allow a large enough ice sheet to remain cold enough to pre-

vent a complete retreat, even during an insolation maximum. At the same time, the presence of a large ice sheet affects atmospheric circulation on the local, regional, and global level. Orographic forcing of precipitation, where air masses moving up the flank of an ice sheet cool down and precipitate their moisture content, results in increased precipitation near the ice-sheet margin, while the interior of the ice sheet becomes a plateau desert (Roe, 2002; Roe & Lindzen, 2001). This does not greatly affect the net mass balance over the entire ice sheet, only the spatial distribution of accumulation. Relatively simple models describing these effects have been shown to produce ice sheets that agree reasonably well with geomorphological evidence of ice-sheet extent (Berends et al., 2018; van den Berg et al., 2008).

Another proposed mechanism for enhanced ice-sheet growth above the lower size threshold involves the topography of North America. Geomorphological evidence indicates that, during the last deglaciation, the North American ice sheet complex separated into the Cordilleran and Laurentide ice sheets (Dyke, 2004). The Laurentide subsequently separated into the Labrador, Keewatin, and Baffin ice sheets, all of which disappeared within a few millennia. Although geomorphological evidence for locations of inception is scarce, model studies (Bahadory et al., 2021; Berends et al., 2018; Calov et al., 2005; Choudhury et al., 2020; de Boer et al., 2013) indicate that glacial inception also occurred separately at all four locations. These models show that, while the Labrador, Keewatin and Baffin ice sheets quickly merged into the Laurentide, the Laurentide and Cordilleran likely did not merge until much later. Bintanja and van de Wal (2008) and Gregoire et al. (2012) suggest that the merging of these two ice sheets presents a strong positive feedback, or even an instability; Bintanja and van de Wal (2008) propose that their merging led to a rapid increase in ice volume with no substantial change in climatic forcing, while Gregoire et al. (2012) show that their separation during the deglaciation led to a rapid retreat. Bintanja and van de Wal (2008) propose that this feedback, and the resulting rapid increase in ice volume, was triggered for the first time during the MPT, when a long-term Pleistocene cooling trend finally resulted in Laurentide and Cordilleran ice sheets that grew large enough to touch, and subsequently merge.

The ice-albedo and elevation-temperature feedbacks are gradual in nature; for these mechanisms, the first size threshold marks the point where the effects of these positive feedbacks become strong enough to negate the melt from an insolation maximum. The merging ice-dome feedback is more abrupt in nature; in this case, the first size threshold directly corresponds to the geographic size required for the separate domes to touch, which is around 45 m of sea level equivalent in North America. Whereas the ice-albedo and elevation-temperature feedbacks are essentially universal, the merging ice-dome feedback is rather a result of the particular topography of the North American continent, making schematic experiments for studying this effect less straightforward.

4.3. Regolith: Basal Sliding and Dust

Clark and Pollard (1998) proposed that the disappearance of the regolith cover beneath the North American and Eurasian ice sheets can explain the MPT. In their theory, before the onset of the Pleistocene glacial cycles, these continents were entirely covered by the thick (10–50 m) layer of regolith that is still found today in the lower-latitude regions that have never been covered by ice sheets. They propose that a regolith substrate easily deforms under the driving stress of an ice sheet, leading to much higher basal velocities than an ice sheet lying on top of hard bedrock. This would lead to the ice sheet being thinner and wider than would be the case under present-day circumstances, in agreement with sparse geological evidence that the pre-MPT Laurentide ice sheet reached a substantially larger extent than during the Last Glacial Maximum (LGM) (Balco & Rovey, 2010; Balco et al., 2005; Boellstorf, 1978). The more gentle surface slopes of this thinner, wider ice sheet would have resulted in a larger ablation zone, which is more sensitive to changes in surface climate. This means that the first size threshold, above which an ice sheet can survive an insolation maximum, lies much higher. They propose that, during the Early Pleistocene, this threshold was never reached, and every insolation maximum led to a deglaciation. However, as the regolith deforms and erodes, it is advected along the direction of ice flow, moving away from the central parts of the glaciated areas. In their theory, the MPT marks the moment when all the regolith was eroded away, and the bare bedrock underneath became exposed. The decrease in basal sliding resulted in ice sheets that were both thicker (providing more stability through the altitude-temperature feedback) and narrower (making them less sensitive to changes in insolation), essentially lowering the first threshold. The ice sheet volume that

could be formed during a single insolation cycle was now large enough to survive an insolation maximum, thus creating the 82/123 kyr glacial cycles of the Late Pleistocene.

Using a coupled ice-sheet – climate – carbon cycle model, Willeit et al. (2019) showed that 100-kyr cycles can occur both with and without a prescribed regolith cover, but that the combination of both a prescribed global cooling trend, and a prescribed gradual removal of regolith during the Pleistocene, gave them the best fit to the observed $\delta^{18}O$ record. However, they still find a maximum ice-sheet extent that is substantially smaller pre-MPT than post-MPT, at odds with the (sparse) geomorphological evidence (Balco & Rovey, 2010; Balco et al., 2005; Boellstorf, 1978).

Regolith erosion has been suggested to influence glacial dynamics not only through reduced basal sliding, but also through its impact on dust fluxes. During the LGM, regolith erosion by the North American ice-sheet complex resulted in increased amounts of atmospheric dust (Kohfeld & Harrison, 2001; McGee et al., 2010). Different studies have suggested that, as some of this dust precipitated onto the ice sheet, the resulting decrease in albedo could have accelerated the retreat of the ice sheet (Peltier & Marshall, 1995; Willeit et al., 2019). In this theory, the MPT is the result of the disappearance of regolith over an increasingly large area of the North American continent, resulting in an increasingly larger ice-sheet size that is required to produce the necessary glaciogenic dust. Proxy data from the North Atlantic support a largely increased glacial dust source from the North American continent starting at 2.7 Myr ago (Naafs et al., 2012). This would be in line with the idea that ice sheets have an impact on dust fluxes. Although the viability of including sediment transport (or tracer tracking in general) in an ice-sheet model has long been demonstrated (Lhomme et al., 2005; Melanson et al., 2013), this has not yet become common practice. Willeit et al. (2019) included glaciogenic dust (using a prescribed regolith mask rather than a transport model), and its effect on both ice-sheet albedo and oceanic productivity, in their coupled ice-sheet – climate – carbon cycle model, but did not explicitly investigate the magnitude of these effects.

4.4. Mechanisms for Increased Sensitivity of Very Large Ice Sheets

The existence of an ice-sheet size threshold required for triggering a termination was already suggested by Raymo (1997). Different mechanisms have been proposed to explain why ice sheets could become more sensitive to changes in insolation when their size exceeds this threshold. Model studies by Abe-Ouchi et al. (2013), Clark and Pollard (1998), and Pollard (1983) suggest that calving might be an important factor. The massive Late Pleistocene ice sheets in North America and Eurasia created deep depressions in the Earth's crust, which, either through oceanic incursion or through the accumulation of meltwater in proglacial lakes, could have resulted in a large portion of the ice-sheet margin becoming marine-based. Clark and Pollard (1998) find that prescribing a sizable calving flux for these marine margins is crucial for achieving a complete deglaciation in their 1-D ice-sheet model. Abe-Ouchi et al. (2013) included, but did not investigate the effect of, a prescribed calving flux in their three-dimensional ice-sheet model. Instead, they suggested that the effect of bedrock depression on the surface mass balance, through the elevation-temperature feedback, is what causes a larger ice sheet to retreat more rapidly. All of these studies prescribed a fixed calving rate for ice margins lying below (local) sea level, implying that calving only occurs when their modeled ice sheet grows large enough to depress the bedrock below sea level or grows off the continental shelf during inception. Furthermore, all of these studies used shallow-ice models, which do not simulate floating ice shelves that might serve as an amplifying factor for ice sheet retreat.

Another proposed mechanism for the reduced stability of large ice sheets involves the thermodynamics of the ice sheet. Bintanja and van de Wal (2008) and Marshall and Clark (2002) propose that the build-up of geothermal heat at the base of an ice-sheet, combined with the insulative properties of the ice, lead to basal temperatures that increase with ice-sheet size. While during the inception phase, the ice sheets are thin enough to remain frozen to the bedrock, they might get thick enough during the glacial highstand to reach pressure melting point at the base, yielding increased basal sliding and rapid thinning of the ice sheet. Clark and Pollard (1998) and Pollard (1983) do not include thermodynamics in their ice-sheet modes, while Abe-Ouchi et al. (2013) include thermodynamics but do not use the resulting basal temperatures to adjust basal friction, such that this feedback process is not present in their models.

5. Non-Ice-Sheet Mechanisms

5.1. Sea Ice

Several other feedback mechanisms have been proposed to explain the existence of 100-kyr glacial cycles, without directly involving ice-sheet dynamics. Gildor and Tziperman (2000, 2001) propose that the growth of sea ice in the Arctic Ocean can act as a climatic "switch," explaining the rapid deglaciations in the Late Pleistocene. They propose that sea ice extent is primarily governed by ocean temperature, which lags atmospheric temperature by several millennia. They also propose that sea ice reduces ocean evaporation, and thereby precipitation over the ice sheets. In the beginning of the inception phase of a glacial cycle, the ocean is still warmer than the atmosphere, so that sea ice extent is small, evaporation is not reduced, and the ice sheets can grow rapidly. Once ocean temperatures drop far enough, the sea ice starts to grow, expanding rapidly due to the ice-albedo feedback (which is even stronger at sea than it is on land). The expanding sea ice cover reduces oceanic evaporation, leading to decreased snow accumulation over the ice sheet. During the deglaciation, the ocean warms more slowly than the atmosphere, maintaining the reduced evaporation and precipitation even as ice sheet melt increases, increasing the rate of retreat. Using a simple box model, they show that this mechanism can produce 100-kyr cycles in response to astronomical forcing. Similar to the nonlinear ice-sheet feedbacks described in the previous section, Gildor and Tziperman (2000, 2001) argue that this mechanism can only act when global temperatures are cold enough for Arctic sea ice to exist at all. A Pleistocene cooling trend could then explain why this was only the case after the MPT.

Gildor and Tziperman (2000, 2001) do not specify a specific latitude for sea ice extent, beyond which accumulation over the ice sheets would be reduced. Proxy data suggest that the Arctic was covered by sea ice throughout the Pleistocene, although earlier in time, for example, before the Mid-Brunhes event (Cronin et al., 2017) or before 1 Myr ago (Detlef et al., 2018) only seasonally. However, recent observations of sea ice extent find a strong correlation to atmospheric temperatures (Olonscheck et al., 2019), casting doubt on the idea of a multi-millennial lag in sea ice extent with respect to changes in atmospheric climate.

5.2. Ocean Circulation and the Carbon Cycle

Several studies have investigated the role of the ocean in the carbon cycle regarding the so-called 100-kyr cycles of the Late Pleistocene. The solubility of CO_2 in the ocean increases with falling sea surface temperatures (SST; Millero, 1995), leading to a strong positive feedback; a global cooling, particularly in (typically high-latitude) locations of deep-water formation, results in an increased uptake of CO_2 by the ocean, reducing the atmospheric CO_2 concentration and reinforcing the cooling. Studies have used coupled ice-sheet – climate – carbon cycle models of intermediate complexity to produce major features of Late Pleistocene atmospheric CO_2 records (Brovkin et al., 2012; Ganopolski & Brovkin, 2017). The most recent application of this type of model covers the entire Pleistocene (Willeit et al., 2019), simulating the reconstructed rise in the glacial/interglacial CO_2 amplitudes across the MPT reasonably well. However, the simulated deglacial CO_2 rise was slower than implied by the data, and the apparent decoupling of CO_2 and temperature/sea level during times of falling obliquity (implying ice-sheet growth) seen in the data (Köhler et al., 2018) has not yet been achieved. Information on carbon isotopes can be used to further evaluate the simulated processes, but since such results have not yet been included in the CLIMBER-2 model version used by Willeit et al. (2019), their results cannot be evaluated from that perspective. Köhler and Bintanja (2008) used a global carbon-cycle box model to investigate why the glacial/interglacial amplitudes in benthic $\delta^{18}O$ increased across the MPT by a factor of two, while those of benthic $\delta^{13}C$ rose by only 20%–40%. Based on their carbon cycle model results, they proposed that, before the MPT, vertical mixing rates in the Southern Ocean were decoupled from SST, while changing as function of SST thereafter. Their simulations show an increase in interglacial atmospheric CO_2 values across the MPT, but no appreciable change in glacial values. This leads to a reduced Early Pleistocene glacial-interglacial (G-IG) CO_2 difference, which agrees with reconstructions based on boron-isotopes (Hönisch et al., 2009). However, the Southern Ocean decoupling hypothesis of Köhler and Bintanja (2008) disagrees in details with the data, since in the reconstructions the glacial CO_2 values decrease across the MPT, but interglacial CO_2 concentrations are similar in pre- and post-MPT times. Furthermore, different studies have reported proxy-based evidence for a systematic change in ocean circulation during the MPT (Hasenfratz et al., 2019; Martínez-Garcia et al., 2010; McClymont et al., 2013; Pena

& Goldstein, 2014), although whether such changes were a cause or a consequence of the MPT remains unclear (Menviel, 2019).

Southern Ocean productivity, and the resulting uptake of atmospheric CO_2, have been directly linked to glaciogenic dust (Martin et al., 1990; Martínez-Garcia et al., 2014). Martin et al. (1990) demonstrated that present-day Antarctic phytoplankton suffer from iron deficiency, resulting in a lower productivity than what could theoretically be achieved with the available sunlight and nutrients. During the LGM, increased glaciogenic dust resulted in iron fertilization of the Southern Ocean, increasing productivity and reducing atmospheric CO_2. Martínez-Garcia et al. (2014) proposed that this positive feedback could have contributed to the self-sustained ice-sheet growth above the first ice-sheet size threshold, explaining how the medium-sized ice-sheets of the Late Pleistocene could survive insolation maxima and achieve their ultimate size. Using a carbon cycle box model, the detected decrease in glacial CO_2 values across the MPT has indeed been attributed to the initiation of substantive dust-borne iron fertilization of marine biology in the Southern Ocean leading to enhanced export production during peak glacial stages (Chalk et al., 2017).

6. Evidence for Long-Term Cooling

Many proposed explanations for the MPT depend on a slow global cooling trend throughout the (Early) Pleistocene, which is usually attributed to a long-term decrease in atmospheric CO_2. Decreased volcanic outgassing (Willeit et al., 2019) and increased weathering (Clark et al., 2006) have been proposed as possible causes of such a trend. In this section, we will review different lines of evidence that could indicate the existence of such a trend.

6.1. Proxy Evidence

A detailed analysis of a large number of proxy-based reconstructions of SST by McClymont et al. (2013) concluded that individual records all showed a gradual cooling across the MPT, but that the timing, the magnitude, and the rate of the cooling varied considerably between records. As few of their records extended beyond 1.5 Myr ago, they did not look for a possible cooling trend throughout the Early Pleistocene. Furthermore, the timing of the transition from 41-kyr to 100-kyr cycles also differed between individual records.

In addition to the SST records compiled in McClymont et al. (2013), we here have a look at benthic $\delta^{18}O$, deep-water temperature, atmospheric CO_2, and benthic $\delta^{13}C$, shown in Figure 5. For the benthic $\delta^{18}O$ stack, peak glacial and interglacial values are marked. Linear trends have been fitted to these peak values both before and after the MPT, as shown by the dashed lines, with the uncertainty in the fits indicated by the shaded areas. During the Early Pleistocene, both glacial and interglacial peak values in benthic $\delta^{18}O$ decrease steadily. After the MPT, the decreasing trend in glacial peak values continues nearly unchanged, while interglacial peak values actually display a slight increase. Since benthic $\delta^{18}O$ contains contributions from both deep-ocean temperature and global ice volume with a temporally variable ratio (de Boer et al., 2013; Elderfield et al., 2012), separating these contributions is not straightforward. Ice-sheet-climate models have been used for this separation of benthic $\delta^{18}O$ (Bintanja & van de Wal, 2008; de Boer et al., 2014; Willeit et al., 2019), finding a gradually increasing contribution of both temperature and sea level change to $\delta^{18}O$ across the MPT, with the larger relative increase in sea level (see Section 5.2 for details).

Elderfield et al. (2012) presented a continuous reconstruction of deep-water temperature going back 1.5 Myr, using the benthic foraminiferal Mg/Ca paleothermometer (Rosenthal et al., 1997). Rohling et al. (2014) used $\delta^{18}O$ in the Mediterranean Sea to reconstruct global mean sea level over the past 5.5 Myr. By subtracting the resulting contribution to global benthic $\delta^{18}O$ from the LR04 stack (Lisiecki & Raymo, 2005), they obtained a global deep-sea temperature reconstruction. The results of these two studies are shown in Figure 5b. Due to the more pronounced interstadials in these reconstructions, pinpointing individual glacials and interglacials and fitting trends to the peak values similar to those in the benthic $\delta^{18}O$ stack is difficult. A sharp temperature decrease is visible around 1,425 kyr ago in the results of Elderfield et al. (2012), after which both peak glacial and interglacial temperatures remain about 1 K below their average Late Pleistocene values for about 200 kyr, all during a period when the benthic $\delta^{18}O$ still shows clear 41-kyr cycles. This appears to conflict with the different hypotheses linking the MPT to a global cooling trend. Rohling et al. (2014) find

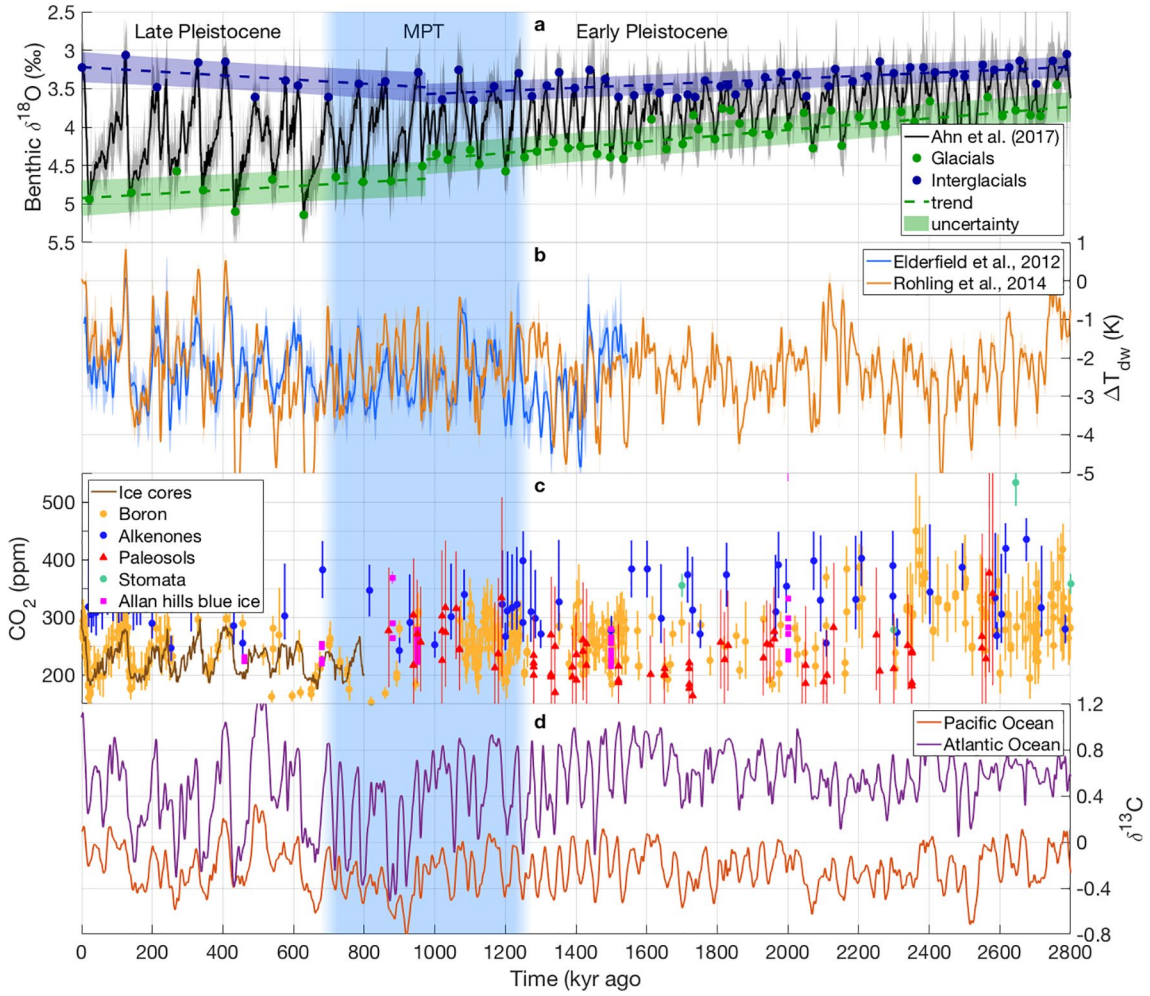

Figure 5. (a) The benthic $\delta^{18}O$ stack by Ahn et al. (2017) (black), with linear trends (dashed lines) fitted to glacial (green) and interglacial (blue) values, both before and after the MPT. Shaded areas indicate the 2σ-range of the linear regression. (b) The deep-water temperature reconstructions based on Mg/Ca ratios by Elderfield et al. (2012) (blue, 5-kyr running mean), and on sea level at the Strait of Gibraltar by Rohling et al. (2014) (orange, 5-kyr running mean). (c) Pleistocene CO_2 proxy data based on ^{11}B ratios (Bartoli et al., 2011; Chalk et al., 2017; Dyez et al., 2018; Hönisch et al., 2009; Martínez-Botí et al., 2015; Seki et al., 2010; Sosdian et al., 2018; Stap et al., 2016; yellow dots), alkenones (Badger et al., 2013; Seki et al., 2010; Zhang et al., 2013; blue dots), paleosols (Da et al., 2019; red triangles), stomata (Bai et al., 2015; Hu et al., 2015; Kürschner et al., 1996; Stults et al., 2011; green dots), the Allan hills blue ice cores (Yan et al., 2019; magenta squares), and the EPICA Dome C ice-core record (Bereiter et al., 2015; brown line). (d) Benthic $\delta^{13}C$ in the Pacific (red, 5-kyr running mean) and Atlantic (purple, 5-kyr running mean) oceans (Lisiecki, 2014).

no such decrease. However, whereas Elderfield et al. (2012) used a global stack of $\delta^{18}O$ from benthic species, Rohling et al. (2014) used only a single core, looking at a planktonic (*G. ruber*) species. This means their data contains a substantial contribution from changes in Mediterranean salinity, which in turn contain a strong precession signal, reflecting regional/seasonal rather than global/annual changes, potentially obscuring the decrease in temperatures observed in the data from Elderfield et al. (2012).

Figure 5c shows the presently available reconstructions of atmospheric CO_2 based on benthic $\delta^{11}B$ (Bartoli et al., 2011; Chalk et al., 2017; Dyez et al., 2018; Hönisch et al., 2009; Martínez-Botí et al., 2015; Seki et al., 2010; Sosdian et al., 2018; Stap et al., 2016), on the ratio of different types of alkenones (Badger et al., 2013; Seki et al., 2010; Zhang et al., 2013), and on the stomatal density of fossil plant leaves (Bai et al., 2015; Hu et al., 2015; Kürschner et al., 1996; Stults et al., 2011), together with the combined ice core record (Bereiter et al., 2015). As can be seen, the proxy records display a large spread and uncertainty, as well as large temporal data gaps. In addition to this, the reliability of both the alkenone and the stomata proxies continues to be contested (Badger et al., 2019; Porter et al., 2019), based mostly on their poor agreement with the ice-core record. The boron isotope data presented by Chalk et al. (2017), which are visible

in Figure 4c as the cluster of data points between 1,250 and 1,075 kyr, shows two 41-kyr cycles, with CO_2 concentrations of 275–325 ppm during the three interglacials, and 200–225 ppm during the two glacials, tentatively supporting the notion of warmer pre-MPT glacials. The data presented by Dyez et al. (2018), visible as the cluster of data points between 1,350 and 1,550 kyr, covers several 41-kyr glacial cycles, but the temporal resolution is too coarse to identify individual glacials or interglacials.

Figure 5d shows benthic $\delta^{13}C$ from the Atlantic and Pacific stacks by Lisiecki (2014), which consist of 39 cores in the Atlantic and seven cores in the Pacific, covering the last 3 Myr. After analyzing these records, Lisiecki (2014) found that Atlantic circulation changed at ~1.5 Myr as a response to obliquity and precession. This agrees with the conclusions of Wang et al. (2010), who analyzed $\delta^{13}C$ from a number of ODP cores in both the Atlantic and Pacific oceans. They found a 400-kyr eccentricity signal in the Early Pleistocene which disappeared around 1.6 Myr, suggesting "a major change in the oceanic carbon reservoir, probably associated with a glacial-induced restructuring of the Southern Ocean" (Wang et al., 2010).

Altogether, some of the available proxy evidence does seem to support a long-term cooling trend. However, reconstructed deep-ocean temperature, atmospheric CO_2, and oceanic $\delta^{13}C$ differ in the details, making it difficult to clearly state which process caused what response.

6.2. Model-Assisted Proxy Data Analysis

The most important and widely used source of information for the Pleistocene is still the benthic $\delta^{18}O$ record, which contains signals from both global ice volume and deep-water temperature. Rather than disentangling these two signals using different proxy data, several studies have attempted to separate the two contributions at the same time with ice-sheet models using an "inverse modeling" approach (e.g., Bintanja & van de Wal, 2008; de Boer et al., 2014). This method derives how global temperatures should have evolved in order to change the global climate, and therefore the evolution of the world's ice sheets, in such a way that they reproduce the observed benthic $\delta^{18}O$ record, using a set of assumptions and empirical relationships between (for example) global surface temperatures, deep-sea temperatures, and benthic $\delta^{18}O$. Furthermore, in an additional step these inverse modeling approaches have also been used to reconstruct the temporal evolution of atmospheric CO_2 across the Pleistocene (Berends et al., 2021; Stap et al., 2018; van de Wal et al., 2011). Van de Wal et al. (2011) calculated CO_2 in post-processing as function of temperature change, while it was directly included in the inverse approach in the other studies. Although these inverse modeling studies are, necessarily, based on simplifications of complex physical processes (e.g., a linearized relation between surface temperatures and deep-sea temperatures, neglecting secondary influences on benthic $\delta^{18}O$ such as changes in ocean pH, etc.; Modestou et al., 2020), their results generally show a good agreement with proxy records of global mean temperature, ice surface temperature, and ice core CO_2 (Berends et al., 2021). An advantage of the approach is that ice volume, temperature, and CO_2 are reconstructed simultaneously, allowing lead-lag relations to be studied without the age model uncertainties present in independent proxy reconstructions. The reconstructed contributions to the benthic $\delta^{18}O$ signal from changes in ice volume and deep-water temperature by Berends et al. (2021) and de Boer et al. (2014) are shown in Figure 6 (while van de Wal et al. (2011) used the same inverse modeling approach, they did not report the separate $\delta^{18}O$ contributions).

Using a different approach, Willeit et al. (2019) used a coupled ice-sheet – climate – carbon cycle model, forced mainly by changes in the orbital parameters (and some assumptions on volcanic CO_2 release), to simulate a history of CO_2. While neither this study, nor the inverse modeling studies, produced perfect reconstructions of atmospheric CO_2, they are all useful for determining the role of different physical processes in the Earth system. The CO_2 histories from these different model studies are shown in Figure 6. The CO_2 reconstruction shown for van de Wal et al. (2011) is an updated version created by Stap et al. (2018), using a new log-linear relationship between (modeled) global mean surface temperature and atmospheric CO_2.

Both Berends et al. (2021) and de Boer et al. (2014) find very similar ice volume contributions to the benthic $\delta^{18}O$ signal (Figure 6a), which is expected since both studies tuned their models to reproduce the sea-level record of the last glacial cycle. The contributions from changes in deep-water temperature (Figure 6b) are less similar, with de Boer et al. (2014) finding substantially larger changes, likely a consequence of the difference in climate forcing between the two studies. Both studies find that the increase in G-IG amplitude

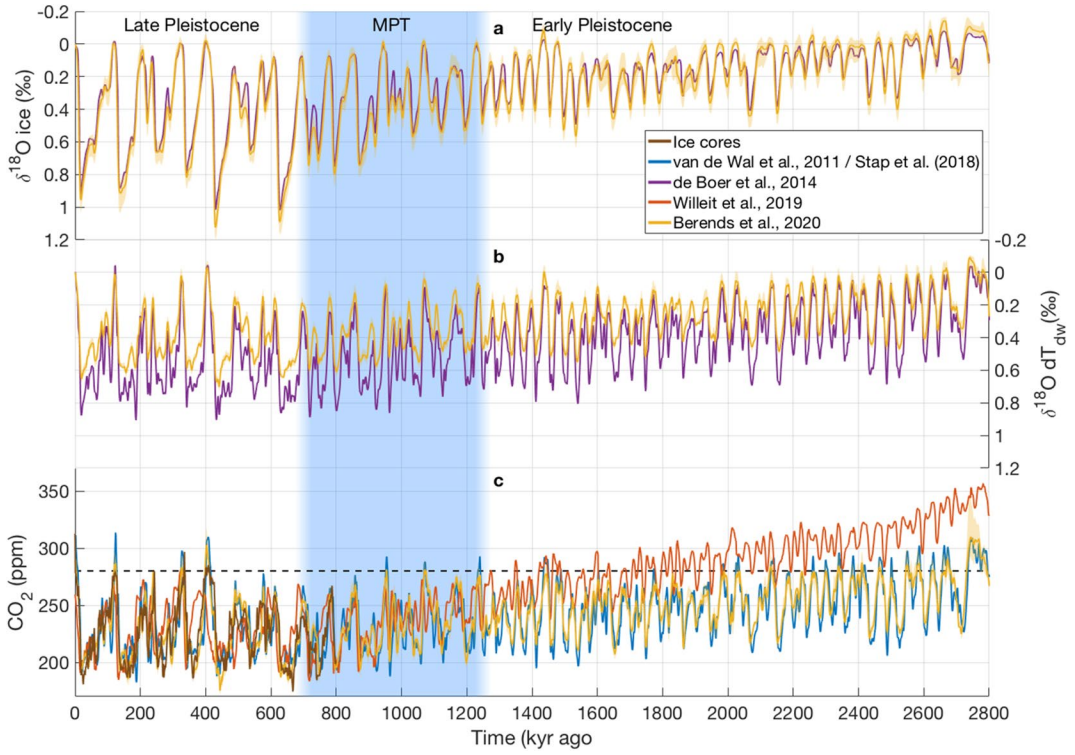

Figure 6. Reconstructed contributions to the benthic $\delta^{18}O$ signal from changes in (a) ice volume and (b) deep-water temperature from the model studies by de Boer et al. (2014) (purple) and Berends et al. (2021) (yellow). (c) Reconstructed CO_2 histories from different model studies, compared to the combined ice core record (Bereiter et al., 2015; brown). van de Wal et al. (2011) (updated by Stap et al., 2018; blue) and Berends et al. (2021) (yellow) used ice-sheet models with parameterized climates, using inverse modeling to reproduce the benthic $\delta^{18}O$ record. Willeit et al. (2019) (red) used a coupled ice-sheet – climate – carbon cycle model, forced with orbital cycles.

during the MPT is mostly a result from an increase in ice volume, with the contribution from deep-water temperature showing a more gradual, long-term decline. Neither van de Wal et al. (2011), or Willeit et al. (2019) reported the separate contributions to the benthic $\delta^{18}O$ signal.

The reconstructed CO_2 histories by Berends et al. (2021), van de Wal et al. (2011), and Willeit et al. (2019) are shown in Figure 6c. During both the MPT and the Late Pleistocene, all three studies show largely the same results, which Berends et al. (2021) showed to be generally in good agreement with the ice-core record. During the Early Pleistocene, the differences between the approaches are more pronounced. The G-IG differences in CO_2 during this period amount to ~65 ppm for van de Wal et al. (2011), ~38 ppm for Willeit et al. (2019), and ~47 ppm for Berends et al. (2021), compared to ~43 ppm suggested by the boron proxy data by Chalk et al. (2017). Willeit et al. (2019) simulates a clearly visible downward trend in the CO_2 concentration throughout the Early Pleistocene. Berends et al. (2021) find a decrease that is much less pronounced, with both glacial and interglacial values decreasing by ~20 ppm between 2.6 and 1.2 Myr ago. Both Berends et al. (2021) and van de Wal et al. (2011) used the LR04 stack (Lisiecki & Raymo, 2005) as forcing for their inverse models, such that the temporal evolution of their CO_2 reconstructions closely reflects the benthic $\delta^{18}O$ record. Willeit et al. (2019) used a much more freely evolving model in that regard, using a carbon-cycle model to simulate CO_2. They attribute the strong downward trend in their results to a prescribed decrease in volcanic CO_2 outgassing during the Pleistocene. Although their simulated CO_2 concentrations during the Early Pleistocene are substantially higher than those of the other approaches (showing a concentration >320 ppm during MIS 110, 2.75 Myr ago), their model set-up still produces sizable ice-sheets during this period, such that their sea-level record (not shown) generally agrees with the other model reconstructions (Berends et al., 2021), as well as the data-based reconstruction by Rohling et al. (2014).

While recent work has greatly increased the amount of CO_2 proxy data (Chalk et al., 2017; Dyez et al., 2018), the sparsity of the data points and the relatively large uncertainties (compared to the continuous, highly accurate ice core record) make meaningful inter-model comparisons difficult. However, the BEOIC project is expected to extend the ice core record to 1.5 Myr ago (Sutter et al., 2019). This will yield a wealth of new information about the MPT, and provide new opportunities for studying the physical mechanisms underlying it. Model studies like those by Berends et al. (2021), van de Wal et al. (2011), and Willeit et al. (2019) are valuable tools for assessing these forthcoming results. For example, Berends et al. (2019) showed that a relatively simple parameterization of the ice-albedo feedback significantly improved the agreement between modeled and observed records of benthic $\delta^{18}O$, ice-core δD, and atmospheric CO_2 during the last four glacial cycles, supporting the hypothesis that this particular feedback process is important in glacial dynamics and can be more constrained once there is a more reliable CO_2 record. Similarly, Willeit et al. (2019) demonstrated that the model-data agreement for benthic $\delta^{18}O$ during the entire Pleistocene was improved when prescribing a gradual removal of regolith and thereby changing the sensitivity of the ice sheets.

7. Summary and Prospects for Future Research

We have reviewed the most important evidence for the existence and nature of the MPT, the different physical mechanisms that have been proposed to explain it, and the proxy evidence for a global cooling trend that is required to activate many of these physical mechanisms. Here, we will summarize our findings, and make some recommendations for future research.

7.1. Nature and Timing

Not all studies that have proposed different physical mechanisms as explanations for the MPT agree on the nature of the Late Pleistocene glacial cycles, either interpreting them as integer multiples of the 41 kyr obliquity cycle (82/123 kyr) or the ~20 kyr precession cycle (80/100/120 kyr), as regular 100 kyr cycles, or even as semi-random fluctuations with no true periodicity. The age models of the proxy archives these studies use to support their hypotheses have uncertainties that are too large to provide a final answer to this question, particularly when considering the fact that these age models are usually orbitally tuned, introducing a problem of circular reasoning (Huybers & Wunsch, 2004). Several studies addressing this problem used simplified box models or 1-D models, forced with the 65°N JJA insolation, which is dominated by the ~20 kyr precession signal. Huybers (2006) argued instead that the ISI is more representative for summer melt than the 65°N JJA insolation, and that the ISI is dominated by the 41 kyr obliquity signal, thus supporting the 82/123 kyr hypothesis. This view is further supported by Tzedakis et al. (2017) by analyzing caloric summer half-year insolation. The simple two-threshold model we present here supports the "orbital pacemaker" hypothesis, where all terminations are caused by insolation maxima (which occur every 41 kyr in our model), but not all insolation maxima cause terminations. In an experiment where we added a small amount of white noise to the sinusoid insolation forcing (10% of the sinusoid amplitude, which can be thought of as internal climate variability), we found that the timing of the terminations is chaotic rather than deterministic. A small change in climate can make the difference between an insolation maximum triggering a termination or merely causing a temporary warm reversal, so that the length of glacial cycles varies arbitrarily between 82 and 123 kyr.

Likewise, studies have proposed a different timing for the MPT, with the differences resulting both from their choice of proxy archives, and their choice of metric for the transition. However, excepting the conceptual models like the one by Paillard (1998) and the one presented here, none of the hypothesized mechanisms for the MPT predict a "hard" transition that can be pinpointed to a single point in time. Rather, all of the "realistic," non-schematic model studies show a "soft" transition, with a gradual deepening of the glacial cycles much like the benthic $\delta^{18}O$ record. This supports the definition of the MPT as a "transition period" (Clark et al., 2006), rather than a single point in time separating the Early and Late Pleistocene.

7.2. Proposed Mechanisms

We have summarized several mechanisms that have been proposed as explanations for the MPT, and formulated a framework of different ice-sheet sensitivity regimes, separated by two thresholds, that can

conceptually accommodate all of these explanations. Comparison of different model results is difficult due to the wide range of model types (box models, one-, two- or three-dimensional ice models, parameterized or modeled climate, prescribed or modeled carbon cycle, etc.), and the fact that there are few models that have studied more than one physical mechanism, and few physical mechanisms that have been studied with more than one model. Furthermore, few of these studies describe in detail which observations might confirm or reject the existence of their proposed mechanism.

The existence of the first ice-sheet size threshold in our framework, which separates small, linearly responding ice sheets from medium-sized, less sensitive ice sheets, is well-supported by the different model studies. Both the ice-albedo feedback and the altitude-temperature feedback are well-established in literature, and have been shown to lead to such a threshold. The merging ice-dome feedback has been less explored, but since it relies on very basic ice sheet dynamics, we believe that this mechanism also played a strong role during the MPT. The physical mechanism behind the second threshold, above which ice sheet sensitivity strongly increases, and an insolation maximum can trigger a termination, is more uncertain. Calving of ice-sheets into proglacial lakes, the link between sediment erosion and basal sliding/surface albedo, and the link between ice-sheet thermodynamics and basal sliding, all seem credible, but the magnitudes of their effects are hard to quantify and difficult to compare. Furthermore, many studies used a benthic $\delta^{18}O$ record as forcing, which means that terminations are already present in the forcing, rather than a consequence of some modeled physical process(es).

7.3. Future Research

The currently ongoing BEOIC project probably presents the most valuable new data to become available in the near future. The different model-based CO_2 reconstructions shown in Figure 6 are not very different in the 800 kyr covered by the EPICA record. In the period between 800 and 1,500 kyr ago (which is aimed to be covered by the new ice core) the differences between the models are much larger. Once this data becomes available, intercomparing the model-data agreements will become much more meaningful. We also believe there is still much to be gained by generating more data with the boron isotope proxy. Currently, the main drawback of this proxy with respect to the ice core record is that the latter presents a continuous record, whereas the former consists of a limited number of single data points. While the error bars of the boron proxy data are also larger, this is mainly due to uncertainties in the conversion from $\delta^{11}B$ to CO_2 concentrations, rather than the measurement uncertainties in $\delta^{11}B$ themselves. This means that these data are still useful to look at relative changes in CO_2, but in order to do that they need to be available at a temporal resolution that is (much) smaller than the half-period of the glacial cycles, so ideally 5 kyr or less. The data produced by Chalk et al. (2017) and Dyez et al. (2018) are a great first step in this direction, and we believe that a continuation of these efforts will be very valuable. Furthermore, the here still existing inconclusiveness of the evidence of a Pleistocene cooling trend needs to be improved by revised and extended proxy data compilations, some of which are already underway (Clark et al., personal communication, 2021).

The lack of a complete understanding of the cause of the MPT also presents an opportunity for new model (intercomparison) studies. A set of standardized schematic experiments that investigate the relevant processes, such that they can be readily performed by different models, could provide valuable new insight into their relative importance in glacial terminations. In particular the effects of calving, thermodynamics, and basal melt on the stability of large ice sheets, need to be studied in more detail than the relatively old, simple experiments that were performed in the original publications proposing these mechanisms. A more coherent effort directed at reproducing these experiments, perhaps in the context of a model intercomparison exercise, could help produce quantitative predictions of the effects of these mechanisms. This can then lead to an improved representation of these processes in more elaborate models, whose results can be compared with proxy reconstructions. The most detailed proxy archives currently available for this purpose are the benthic $\delta^{18}O$ record, and the ice-core CO_2 record. This means it would also be useful to direct more effort at model-data integration. Studies like Clarke et al. (2005), Lhomme et al. (2005), and Melanson et al. (2013) show that it is not particularly complicated to add modules for isotope/tracer tracking or sediment transport to ice-sheet models. In the last few years, several modeling groups have worked on developing coupled or hybrid ice/climate models that are capable of simulating glacial cycles, but the inclusion of such modules

into these models is not yet commonplace. However, this would allow one to compare modeled and observed benthic $\delta^{18}O$ records, sediment cores, or ice cores and is thereby very useful.

Many of these paleo-ice-sheet models use either benthic $\delta^{18}O$ or ice-core CO_2 as forcing. Since glacial cycles are already present in these records, using them as forcing defeats the purpose of studying the dynamics of terminations. We therefore believe the best approach is that taken by Willeit et al. (2019), where insolation is prescribed as forcing, and a carbon cycle model is used to simulate CO_2. However, their model set-up includes an elaborate climate component, the intermediate-complexity model CLIMBER-2, which might not be necessary, since few of the physical mechanisms described here involve atmospheric processes (excepting the ice-albedo, altitude-temperature and orographic precipitation feedbacks, which Berends et al. (2018) showed to be well-captured in some parameterized models). In order to save on computational resources and overall research effort, it might therefore be more practical to create a model set-up that uses a more simplified climate component, such as the matrix method developed by Berends et al. (2018, 2021), which uses relatively simple, computationally efficient parameterizations to combine output from pre-calculated GCM simulations, combined with the carbon-cycle – ice-sheet model coupling used by Willeit et al. (2019). Such a model set-up will be computationally fast enough to allow for the kind of ensemble simulations required for studying the impacts of the different physical processes proposed as explanations for the second threshold. If this hypothetical model set-up includes the ability to predict both $\delta^{18}O$ and CO_2, it would be able to provide ample opportunity for model-data comparisons, possibly settling the question of what caused the MPT.

Lastly, we believe the spatial variability of different proxies could be studied in more detail, and used for the calibration of models. Whereas the CO_2 concentration in the atmosphere is essentially uniform, substantial spatial variation exists in quantities like ocean salinity, ocean temperature (both surface and deep waters), and benthic $\delta^{18}O$ and $\delta^{13}C$. A lot of the model/data comparisons currently look only at global averages, which could be an oversimplification. While this certainly presents a challenge to modelers, we believe the results could be very valuable and contribute to unraveling the MPT enigma.

Appendix A: A Two-Threshold Model

In order to demonstrate of conceptual response of the simplified two-threshold framework illustrated in Figure 4, we constructed a simple zero-dimensional model. "Ice-sheet size" is described by the scalar variable V (expressed in meters of sea-level equivalent, m.s.l.e), which is solved forward through time with a 1 kyr time step. The two thresholds are fixed at $V = 50$ m and $V = 90$ m, respectively. The "mass balance" $\frac{dV}{dt}$ (in m.s.l.e yr^{-1}) is a function of the "insolation" $Q(t)$ (normalized to zero mean and unit variance) and the ice-sheet size V, depending on the ice-sheet size regime:

$$\frac{dV}{dt} = \begin{cases} -3Q(t) & \text{if } V < 50 \\ 1 - 2Q(t) & \text{if } V \geq 50 \end{cases} \tag{A1}$$

The first case describes the "small" regime, where the mass balance depends linearly on the insolation. The second case describes the "medium" regime, where the sensitivity to insolation is reduced, and a small added constant describes the self-sustained growth resulting from some positive feedback. If $V > 90$ m, a termination is triggered and the mass balance is set to $\frac{dV}{dt} = -18$ m yr^{-1} until $V = 0$ m. The model is forced with a simple 41-kyr sinusoid insolation function, plus a small, linear cooling trend, such that $Q(t) = \sin\frac{2\pi t}{41{,}000} + 0.2 - \frac{t}{5{,}000{,}000}$.

Data Availability Statement

No new data were used or created for this research.

Acknowledgments
This publication was generated in the frame of Beyond EPICA. The project has received funding from the European Union's Horizon 2020 research and innovation program under grant agreement No. 815384 (Oldest Ice Core). It is supported by national partners and funding agencies in Belgium, Denmark, France, Germany, Italy, Norway, Sweden, Switzerland, The Netherlands, and the United Kingdom. Logistic support is mainly provided by PNRA and IPEV through the Concordia Station system. The opinions expressed and arguments employed herein do not necessarily reflect the official views of the European Union funding agency or other national funding bodies. This is Beyond EPICA publication number 18.

References

Abe-Ouchi, A., Saito, F., Kawamura, K., Raymo, M. E., Okuno, J., Takahashi, K., & Blatter, H. (2013). Insolation-driven 100,000-year glacial cycles and hysteresis of ice-sheet volume. *Nature*, *500*, 190–193. https://doi.org/10.1038/nature12374

Ahn, S., Khider, D., Lisiecki, L. E., & Lawrence, C. E. (2017). A probabilistic Pliocene-Pleistocene stack of benthic d18O using a profile hidden Markov model. *Dynamics and Statistics of the Climate System*, *2*, 1–16. https://doi.org/10.1093/climsys/dzx002

Badger, M. P. S., Chalk, T. B., Foster, G. L., Brown, P. R., Gibbs, S. J., Sexton, P. F., et al. (2019). Insensitivity of alkenone carbon isotopes to atmospheric CO_2 at low to moderate CO_2 levels. *Climate of the Past*, *15*, 539–554. https://doi.org/10.5194/cp-15-539-2019

Badger, M. P. S., Schmidt, D. N., Mackensen, A., & Pancost, R. D. (2013). High-resolution alkenone palaeobarometry indicates relatively stable pCO_2 during the Pliocene (3.3-2.8 Ma). *Philosophical Transactions of the Royal Society A*, *371*. https://doi.org/10.1098/rsta.2013.0094

Bahadory, T., Tarasov, L., & Andres, H. (2021). Last glacial inception trajectories for the Northern Hemisphere from coupled ice and climate modeling. *Climate of the Past*, *17*, 397–418. https://doi.org/10.5194/cp-17-397-2021

Bai, Y.-J., Chen, L.-Q., Ranhotra, P. S., Wang, Q., Wang, Y.-F., & Li, C.-S. (2015). Reconstructing atmospheric CO_2 during the Plio-Pleistocene transition by fossil Typha. *Global Change Biology*, *21*, 874–881. https://doi.org/10.1111/gcb.12670

Balco, G., & Rovey, C. W. (2010). Absolute chronology for major Pleistocene advances of the Laurentide Ice Sheet. *Geology*, *38*, 795–798. https://doi.org/10.1130/g30946.1

Balco, G., Rovey, C. W., & Stone, J. O. H. (2005). The first glacial maximum in North America. *Science*, *307*, 222–222. https://doi.org/10.1126/science.1103406

Barnola, J.-M., Raynaud, D., Korotkevich, Y. S., & Lorius, C. (1987). Vostok ice core provides 160,000-year record of atmospheric CO_2. *Nature*, *329*, 408–414. https://doi.org/10.1038/329408a0

Bartoli, G., Hönisch, B., & Zeebe, R. E. (2011). Atmospheric CO_2 decline during the Pliocene intensification of Northern Hemisphere glaciations. *Paleoceanography*, *26*.

Bassinot, F. C., Labeyrie, L. D., Vincent, E., Quidelleur, X., Shackleton, N. J., & Lancelot, Y. (1994). The astronomical theory of climate and the age of the Brunhes-Matuyama magnetic reversal. *Earth and Planetary Science Letters*, *126*, 91–108. https://doi.org/10.1016/0012-821x(94)90244-5

Bazin, L., Landais, A., Lemieux-Dudon, B., Toyé Mahamadou Kele, H., Veres, D., Parrenin, F., et al. (2013). An optimized multi-proxy, multi-site Antarctic ice and gas orbital chronology (AICC2012): 120-800 ka. *Climate of the Past*, *9*, 1715–1731. https://doi.org/10.5194/cp-9-1715-2013

Bereiter, B., Eggleston, S., Schmitt, J., Nehrbass-Ahles, C., Stocker, T. F., Fischer, H., et al. (2015). Revision of the EPICA Dome C CO_2 record from 800 to 600 kyr before present. *Geophysical Research Letters*, *42*, 542–549. https://doi.org/10.1002/2014gl061957

Berends, C. J., des Boer, B., Dolan, A. M., Hill, D. J., & van de Wal, R. S. W. (2019). Modeling ice sheet evolution and atmospheric CO_2 during the Late Pliocene. *Climate of the Past*, *15*, 1603–1619. https://doi.org/10.5194/cp-15-1603-2019

Berends, C. J., de Boer, B., & van de Wal, R. S. W. (2018). Application of HadCM3@Bristolv1.0 simulations of paleoclimate as forcing for an ice-sheet model, ANICE2.1: Set-up and benchmark experiments. *Geoscientific Model Development*, *11*, 4657–4675. https://doi.org/10.5194/gmd-11-4657-2018

Berends, C. J., de Boer, B., & van de Wal, R. S. W. (2021). Reconstructing the evolution of ice sheets, sea level, and atmospheric CO_2 during the past 3.6 million years. *Climate of the Past*, *17*, 361–377. https://doi.org/10.5194/cp-17-361-2021

Bintanja, R., & van de Wal, R. S. W. (2008). North American ice-sheet dynamics and the onset of 100,000-year glacial cycles. *Nature*, *454*, 869–872. https://doi.org/10.1038/nature07158

Boellstorf, J. (1978). North American Pleistocene stages reconsidered in light of probably Pliocene-Pleistocene Continental Glaciation. *Science*, *202*, 305–307. https://doi.org/10.1126/science.202.4365.305

Brovkin, V., Ganopolski, A., Archer, D., & Munhoven, G. (2012). Glacial CO_2 cycle as a succession of key physical and biogeochemical processes. *Climate of the Past*, *8*, 251–264. https://doi.org/10.5194/cp-8-251-2012

Budyko, M. I. (1969). The effect of solar radiation variations on the climate of the Earth. *Tellus*, *21*, 611–619. https://doi.org/10.3402/tellusa.v21i5.10109

Calov, R., Ganopolski, A., Claussen, M., Petoukhov, V., & Greve, R. (2005). Transient simulation of the last glacial inception. Part I: Glacial inception as a bifurcation in the climate system. *Climate Dynamics*, *24*, 545–561. https://doi.org/10.1007/s00382-005-0007-6

Chalk, T. B., Hain, M. P., Foster, G. L., Rohling, E. J., Sexton, P. F., Badger, M. P. S., et al. (2017). Causes of ice age intensification across the Mid-Pleistocene Transition. *Proceedings of the National Academy of Sciences*, *114*, 13114–13119. https://doi.org/10.1073/pnas.1702143114

Choudhury, D., Timmermann, A., Schloesser, F., Heinemann, M., & Pollard, D. (2020). Simulating Marine Isotope Stage 7 with a coupled climate-ice sheet model. *Climate of the Past*, *16*, 2183–2201. https://doi.org/10.5194/cp-16-2183-2020

Clarke, G. K. C., Lhomme, N., & Marshall, S. J. (2005). Tracer transport in the Greenland ice sheet: Three-dimensional isotopic stratigraphy. *Quaternary Science Reviews*, *24*, 155–171. https://doi.org/10.1016/j.quascirev.2004.08.021

Clark, P. U., Archer, D., Pollard, D., Blum, J. D., Rial, J. A., Brovkin, V., et al. (2006). The middle Pleistocene transition: Characteristics, mechanisms, and implications for long-term changes in atmospheric pCO_2. *Quaternary Science Reviews*, *25*, 3150–3184. https://doi.org/10.1016/j.quascirev.2006.07.008

Clark, P. U., & Pollard, D. (1998). Origin of the middle Pleistocene transition by ice sheet erosion of regolith. *Paleoceanography*, *13*, 1–9. https://doi.org/10.1029/97pa02660

Cronin, T. M., Dwyer, G. S., Caverly, E. K., Farmer, J., DeNinno, L. H., Rodriguez-Lazaro, J., & Gemery, L. (2017). Enhanced Arctic amplification began at the Mid-Brunhes event ~400,000 years ago. *Scientific Reports*, *7*. https://doi.org/10.1038/s41598-017-13821-2

Da, J., Zhang, Y. G., Li, G., Meng, X., & Ji, J. (2019). Low CO_2 levels of the entire Pleistocene epoch. *Nature Communications*, *10*. https://doi.org/10.1038/s41467-019-12357-5

Dansgaard, W. (1964). Stable isotopes in precipitation. *Tellus*, *16*, 436–468. https://doi.org/10.3402/tellusa.v16i4.8993

de Boer, B., Lourens, L. J., & van de Wal, R. S. W. Persistent 400,000-year variability of Antarctic ice volume and the carbon cycle is revealed throughout the Plio-Pleistocene. *Nature Communications*, *5*, 2014.

de Boer, B., van de Wal, R., Lourens, L. J., Bintanja, R., & Reerink, T. J. (2013). A continuous simulation of global ice volume over the past 1 million years with 3-D ice-sheet models. *Climate Dynamics*, *41*, 1365–1384. https://doi.org/10.1007/s00382-012-1562-2

Detlef, H., Belt, S. T., Sosdian, S. M., Smik, L., Lear, C. H., Hall, I. R., et al. (2018). Sea ice dynamics across the Mid-Pleistocene transition in the Bering Sea. *Nature Communications*, *9*. https://doi.org/10.1038/s41467-018-02845-5

Dyez, K. A., Hönisch, B., & Schmidt, G. A. (2018). Early Pleistocene obliquity-scale pCO2 variability at ~1.5 milion years ago. *Paleoceanography and Paleoclimatology*, *33*, 1270–1291. https://doi.org/10.1029/2018pa003349

Dyke, A. S. (2004). An outline of North American deglaciation with emphasis on central and northern Canada. *Quaternary Glaciations – Extent and Chronology, Part II*, 373–424.
Elderfield, H., Ferretti, P., Greaves, M., Crowhurst, S., McCave, I. N., Hodell, D. A., & Piotrowski, A. M. (2012). Evolution of ocean temperature and ice volume through the mid-Pleistocene climate transition. *Science*, *337*, 704–709. https://doi.org/10.1126/science.1221294
EPICA Community members. (2004). Eight glacial cycles from an Antarctic ice core. *Nature*, *429*, 623–628.
Fleming, J. R. (2006). James croll in context: The encounter between climate dynamics and geology in the second half of the nineteenth century. *History of Meteorology*, *3*, 43–54.
Ganopolski, A., & Brovkin, V. (2017). Simulation of climate, ice sheets and CO2 evolution during the last four glacial cycles with an Earth system model of intermediate complexity. *Climate of the Past*, *13*, 1695–1716. https://doi.org/10.5194/cp-13-1695-2017
Ganopolski, A., & Calov, R. (2011). The role of orbital forcing, carbon dioxide and regolith in 100 kyr glacial cycles. *Climate of the Past*, *7*, 1415–1425. https://doi.org/10.5194/cp-7-1415-2011
Gildor, H., & Tziperman, E. (2000). Sea ice as the glacial cycles' climate switch: Role of seasonal and orbital forcing. *Paleoceanography*, *15*, 605–615. https://doi.org/10.1029/1999pa000461
Gildor, H., & Tziperman, E. (2001). A sea ice climate switch mechanism for the 100-kyr glacial cycles. *Journal of Geophysical Research*, *106*, 9117–9133. https://doi.org/10.1029/1999jc000120
Gregoire, L. J., Payne, A. J., & Valdes, P. J. (2012). Deglacial rapid sea level rises caused by ice-sheet saddle collapses. *Nature Letters*, *487*, 219–222. https://doi.org/10.1038/nature11257
Hasenclever, J., Knorr, G., Rüpke, L. H., Köhler, P., Morgan, J., Garofalo, K., et al. (2017). Sea level fall during deglaciation stabilized atmospheric CO_2 by enhanced volcanic degassing. *Nature Communications*, *8*. https://doi.org/10.1038/ncomms15867
Hasenfratz, A. P., Jaccard, S. L., Martínez-García, A., Sigman, D. M., Hodell, D. A., Vance, D., et al. (2019). The residence time of Southern Ocean surface waters and the 100,000-year ice age cycle. *Science*, *363*, 1080–1084. https://doi.org/10.1126/science.aat7067
Hays, J. D., Imbrie, J., & Shackleton, N. J. (1976). Variations in the Earth's orbit: Pacemaker of the Ice Ages. *Science*, *194*, 1121–1132. https://doi.org/10.1126/science.194.4270.1121
Hönisch, B., Hemming, N. G., Archer, D., Siddall, M., & McManus, J. F. (2009). Atmospheric carbon dioxide concentration across the mid-Pleistocene transition. *Science*, *324*, 1551–1554. https://doi.org/10.1126/science.1171477
Hu, J.-J., Xing, Y.-W., Turkington, R., Jacques, F. M. B., Su, T., Huang, Y.-J., & Zhou, Z.-K. (2015). A new positive relationship between pCO_2 and stomatal frequency in Quercus guyavifolia (Fagaceae): A potential proxy for palaeo-CO_2 levels. *Annals of Botany*, *115*, 777–788. https://doi.org/10.1093/aob/mcv007
Huybers, P. (2006). Early Pleistocene glacial cycles and the integrated summer insolation forcing. *Science*, *313*. https://doi.org/10.1126/science.1125249
Huybers, P. (2007). Glacial variability of the last two million years: An extended depth-derived age model, continuous obliquity pacing, and the Pleistocene progression. *Quaternary Science Reviews*, *26*, 37–55. https://doi.org/10.1016/j.quascirev.2006.07.013
Huybers, P. (2011). Combined obliquity and precession pacing of late Pleistocene glaciations. *Nature*, *480*, 229–232. https://doi.org/10.1038/nature10626
Huybers, P., & Wunsch, C. (2004). A depth-derived Pleistocene age model: Uncertainty estimates, sedimentation variability, and nonlinear climate change. *Paleoceanography*, *19*. https://doi.org/10.1029/2002pa000857
Huybers, P., & Wunsch, C. (2005). Obliquity pacing of the late Pleistocene glacial terminations. *Nature*, *434*, 491–494. https://doi.org/10.1038/nature03401
Imbrie, J., Hays, J. D., Martinson, D. G., McIntyre, A., Mix, A. C., Morley, J. J., et al. (1984). The orbital theory of Pleistocene climate: Support from a revised chronology of the marine $\delta^{18}O$ record. *Milankovitch and Climate*: Understanding the response to astronomical forcing, *1*, 269–305.
Imbrie, J. Z., Imbrie-Moore, A., & Lisiecki, L. E. (2011). A phase-space model for Pleistocene ice volume. *Earth and Planetary Science Letters*, *307*, 94–102. https://doi.org/10.1016/j.epsl.2011.04.018
Jouzel, J., Alley, R. B., Cuffey, K. M., Dansgaard, W., Grootes, P., Hoffmann, G., et al. (1997). Validity of the temperature reconstruction from water isotopes in ice cores. *Journal of Geophysical Research*, *102*, 26471–26487. https://doi.org/10.1029/97jc01283
Jouzel, J., Masson-Delmote, V., Cattani, O., Dreyfus, G., Falourd, S., Hoffmann, G., et al. (2007). Orbital and Millennial Antarctic climate variability over the past 800,000 years. *Science*, *317*, 793–796. https://doi.org/10.1126/science.1141038
Karner, D. B., Levine, J., Medeiros, B. P., & Muller, R. A. (2002). Constructing a stacked benthic d18O record. *Paleoceanography*, *17*. https://doi.org/10.1029/2001pa000667
Kohfeld, K. E., & Harrison, S. P. (2001). DIRTMAP: The geological record of dust. *Earth-Science Reviews*, *54*, 81–114. https://doi.org/10.1016/s0012-8252(01)00042-3
Köhler, P., & Bintanja, R. (2008). The carbon cycle during the Mid Pleistocene Transition: The Southern Ocean decoupling hypothesis. *Climate of the Past*, *4*, 311–332. https://doi.org/10.5194/cp-4-311-2008
Köhler, P., Knorr, G., Stap, L. B., Ganopolski, A., de Boer, B., van de Wal, R. S. W., et al. (2018). The effect of obliquity-driven changes on paleoclimate sensitivity during the Late Pleistocene. *Geophysical Research Letters*, *45*, 6661–6671. https://doi.org/10.1029/2018gl077717
Köhler, P., & van de Wal, R. S. W. (2020). Interglacials of the Quaternary defined by northern hemispheric land ice distribution outside of Greenland. *Nature Communications*, *11*, 5124. https://doi.org/10.1038/s41467-020-18897-5
Konijnendijk, T. Y. M., Ziegler, M., & Lourens, L. J. (2015). On the timing and forcing mechanisms of late Pleistocene glacial terminations: Insights from a new high-resolution benthic stable oxygen isotope record of the eastern Mediterranean. *Quaternary Science Reviews*, *129*, 308–320. https://doi.org/10.1016/j.quascirev.2015.10.005
Kürschner, W. M., van der Burgh, J., Visscher, H., & Dilcher, D. L. (1996). Oak leaves as biosensors of late Neogene and early Pleistocene paleoatmosphere CO2 concentrations. *Marine Micropaleontology*, *27*, 299–312. https://doi.org/10.1016/0377-8398(95)00067-4
Laskar, J., Robutel, P., Gastineau, M., Correia, A. C. M., Levrard, B., & Levrard, B. (2004). A long-term numerical solution for the insolation quantities of the Earth. *Astronomy & Astrophysics*, *428*, 261–285. https://doi.org/10.1051/0004-6361:20041335
Lhomme, N., Clarke, G. K. C., & Marshall, S. J. (2005). Tracer transport in the Greenland Ice Sheet: Constraints on ice cores and glacial history. *Quaternary Science Reviews*, *24*, 173–194. https://doi.org/10.1016/j.quascirev.2004.08.020
Lisiecki, L. E. (2010). Links between eccentricity forcing and the 100,000-year glacial cycle. *Nature Geoscience*, *3*, 349–352. https://doi.org/10.1038/ngeo828
Lisiecki, L. E. (2014). Atlantic overturning responses to obliquity and precession over the last 3 Myr. *Paleoceanography*, *29*, 71–86. https://doi.org/10.1002/2013pa002505
Lisiecki, L. E., & Raymo, M. E. (2005). A Pliocene-Pleistocene stack of 57 globally distributed benthic delta-18-O records. *Paleoceanography*, *20*. https://doi.org/10.1029/2004pa001071

Liu, Z., Cleaveland, L. C., & Herbert, T. D. (2008). Early onset and origin of 100-kyr cycles in Pleistocene tropical SST records. *Earth and Planetary Science Letters*, *265*, 703–715. https://doi.org/10.1016/j.epsl.2007.11.016

Lourens, L. J., Becker, J., Bintanja, R., Hilgen, F. J., Tuenter, E., van de Wal, R. S. W., & Ziegler, M. (2010). Linear and non-linear response of late Neogene glacial cycles to obliquity forcing and implications for the Milankovitch theory. *Quaternary Science Reviews*, *29*, 352–365. https://doi.org/10.1016/j.quascirev.2009.10.018

Marshall, S. J., & Clark, P. U. (2002). Basal temperature evolution of North American ice sheets and implications for the 100-kyr cycle. *Geophysical Research Letters*, *29*. https://doi.org/10.1029/2002gl015192

Martin, J. H., Gordon, R. M., & Fitzwater, S. E. (1990). Iron in Antarctic waters. *Nature*, *345*, 156–158. https://doi.org/10.1038/345156a0

Martinez-Boti, M. A., Foster, G. L., Chalk, T. B., Rohling, E. J., Sexton, P. F., Lunt, D. J., et al. (2015). Plio-Pleistocene climate sensitivity evaluated using high-resolution CO_2 records. *Nature*, *518*, 49–54. https://doi.org/10.1038/nature14145

Martínez-García, A., Rosell-Melé, A., McClymont, E. L., Gersonde, R., & Haug, G. H. (2010). Subpolar link to the emergence of the Modern Equatorial Pacific Cold Tongue. *Science*, *328*, 1550–1553. https://doi.org/10.1126/science.1184480

Martínez-García, A., Sigman, D. M., Ren, H., Anderson, R. F., Straub, M., Hodell, D. A., et al. (2014). Iron fertilization of the Subantarctic Ocean during the Last Ice Age. *Science*, *343*, 1347–1350. https://doi.org/10.1126/science.1246848

McClymont, E. L., Sosdian, S. M., Rosell-Melé, A., & Rosenthal, Y. (2013). Pleistocene sea-surface temperature evolution: Early cooling, delayed glacial intensification, and implications for the mid-Pleistocene climate transition. *Earth-Science Reviews*, *123*, 173–193. https://doi.org/10.1016/j.earscirev.2013.04.006

McGee, D., Broecker, W. S., & Winckler, G. (2010). Gustiness: The driver of glacial dustiness? *Quaternary Science Reviews*, *29*, 2340–2350. https://doi.org/10.1016/j.quascirev.2010.06.009

Melanson, A., Bell, T., & Tarasov, L. (2013). Numerical modeling of subglacial erosion and sediment transport and its application to the North American ice sheets over the Last Glacial cycle. *Quaternary Science Reviews*, *68*, 154–174. https://doi.org/10.1016/j.quascirev.2013.02.017

Menviel, L. (2019). The southern amplifier. *Science*, *363*, 1040–1041. https://doi.org/10.1126/science.aaw7196

Milankovic, M. (1941). *Kanon der Erdbestrahlung und seine Anwendung auf das Eiszeitenproblem*.

Millero, F. J. (1995). Thermodynamics of the carbon dioxide system in the oceans. *Geochimica et Cosmochimica Acta*, *59*, 661–677. https://doi.org/10.1016/0016-7037(94)00354-o

Modestou, S. E., Leutert, T. J., Fernandez, A., Lear, C. H., & Meckler, A. N. (2020). Warm middle Miocene Indian Ocean bottom water temperatures: Comparison of clumped isotope and Mg/Ca based estimates. *Paleoceanography and Paleoclimatology*.

Naafs, B. D. A., Hefter, J., Acton, G., Haug, G. H., Martínez-García, A., Pancost, R. D., & Stein, R. (2012). Strengthening of North American dust sources during the late Pliocene (2.7 Ma). *Earth and Planetary Science Letters*, *317–318*, 8–19. https://doi.org/10.1016/j.epsl.2011.11.026

Nyman, K. H. M., & Ditlevsen, P. D. (2019). The middle Pleistocene transition by frequency locking and slow ramping of internal period. *Climate Dynamics*, *53*, 3023–3038. https://doi.org/10.1007/s00382-019-04679-3

Oerlemans, J. (1980). Model experiments on the 100,000-yr glacial cycle. *Nature*, *287*, 430–432. https://doi.org/10.1038/287430a0

Olonscheck, D., Mauritsen, T., & Notz, D. (2019). Arctic sea-ice variability is primarily driven by atmospheric temperature fluctuations. *Nature Geoscience*, *12*, 430–434. https://doi.org/10.1038/s41561-019-0363-1

Oppenheimer, M., Glavovic, B., Hinkel, J., van de Wal, R. S. W., Magnan, A. K., Abd-Elgawad, A., et al. (2019). Sea level rise and implications for low lying islands, coasts, and communities. In D. C. Roberts, V. Masson-Delmotte, P. Zhai, M. Tignor, E. Poloczanska, K. Mintenbeck, M. Nicolai, A. Okem, J. Petzold, B. Rama, & N. Weyer (Eds.), *IPCC special report on the ocean and cryosphere in a changing climate [H.-O. Pörtner]*.

Paillard, D. (1998). The timing of Pleistocene glaciations from a simple multiple-state climate model. *Nature*, *391*, 378–381. https://doi.org/10.1038/34891

Paillard, D. (2001). Glacial cycles: Toward a new paradigm. *Reviews of Geophysics*, *39*, 325–346. https://doi.org/10.1029/2000rg000091

Past Interglacials Working Group of PAGES. (2016). Interglacials of the last 800,000 years. *Reviews of Geophysics*, *54*, 162–219.

Peltier, W. R., & Marshall, S. J. (1995). Coupled energy-balance/ice-sheet model simulations of the glacial cycle: A possible connection between terminations and terrigenous dust. *Journal of Geophysical Research*, *100*, 14269–14289.

Pena, L. D., & Goldstein, S. L. (2014). Thermohaline circulation crisis and impacts during the mid-Pleistocene transition. *Science*, *345*, 318–322. https://doi.org/10.1126/science.1249770

Pisias, N. G., Martinson, D. G., Moore, T. C., Shackleton, N. J., Prell, W., Hays, J. D., & Boden, G. (1984). High resolution stratigraphic correlation of benthic oxygen isotopic records spanning the last 300,000 years. *Marine Geology*, *56*, 119–136. https://doi.org/10.1016/0025-3227(84)90009-4

Pisias, N. G., & Moore, T. C. (1981). The evolution of Pleistocene climate: A time series approach. *Earth and Planetary Science Letters*, *52*, 450–458. https://doi.org/10.1016/0012-821x(81)90197-7

Pollard, D. (1983). A coupled Climate-Ice Sheet model applied to the Quaternary Ice Ages. *Journal of Geophysical Research*, *88*, 7705–7718. https://doi.org/10.1029/jc088ic12p07705

Porter, A. S., Evans-FitsGerald, C., Yiotis, C., Montañez, I. P., & McElwain, J. C. (2019). Testing the accuracy of new paleoatmosphere CO_2 proxies based on plant stable isotopic composition and stomatal traits in a range of simulated paleoatmosphere O2: CO2 ratios. *Geochimica et Cosmochimica Acta*, *259*, 69–90. https://doi.org/10.1016/j.gca.2019.05.037

Prell, W. L., Imbrie, J., Martinson, D. G., Morley, J. J., Pisias, N. G., Shackleton, N. J., & Streeter, H. F. (1986). Graphic correlation of oxygen isotope stratigraphy application to the late Quaternary. *Paleoceanography*, *1*, 137–162. https://doi.org/10.1029/pa001i002p00137

Raymo, M. E. (1997). The timing of major climate terminations. *Paleoceanography*, *12*, 577–585. https://doi.org/10.1029/97pa01169

Raymo, M. E., Ruddiman, W. F., Shackleton, N. J., & Oppo, D. W. (1990). Evolution of Atlantic-Pacific d13C gradients over the last 2.5 m.y. *Earth and Planetary Science Letters*, *97*, 353–368. https://doi.org/10.1016/0012-821x(90)90051-x

Ridgwell, A. J., Watson, A. J., & Raymo, M. E. (1999). Is the spectral signature of the 100 kyr glacial cycle consistent with a Milankovitch origin? *Paleoceanography*, *14*, 437–440. https://doi.org/10.1029/1999pa900018

Roe, G. H. (2002). Modeling precipitation over ice sheets: An assessment using Greenland. *Journal of Glaciology*, *48*, 70–80. https://doi.org/10.3189/172756502781831593

Roe, G. H., & Lindzen, R. S. (2001). The mutual interaction between Continental-Scale Ice Sheets and atmospheric stationary waves. *Journal of Climate*, *14*, 1450–1465. https://doi.org/10.1175/1520-0442(2001)014<1450:tmibcs>2.0.co;2

Rohling, E. J., Foster, G. L., Marino, G., Roberts, A. P., Tamisiea, M. E., Williams, F., & Williams, F. (2014). Sea-level and deep-sea-temperature variability over the past 5.3 million years. *Nature*, *508*, 477–482. https://doi.org/10.1038/nature13230

Rosenthal, Y., Boyle, E. A., & Slowey, N. (1997). Temperature control on the incorporation of magnesium, strontium, fluorine and cadmium into benthic foraminiferal shells from Little Bahama Bank: Prospects for thermocline paleoceanography. *Geochimica et Cosmochimica Acta*, *61*, 3633–3643. https://doi.org/10.1016/s0016-7037(97)00181-6

Rutherford, S., & D'Hondt, S. (2000). Early onset and tropical forcing of 100,000-year Pleistocene glacial cycles. *Nature*, *408*, 72–75. https://doi.org/10.1038/35040533

Schulz, K. G., & Zeebe, R. E. (2006). Pleistocene glacial terminations triggered by synchronous changes in Southern and Northern Hemisphere insolation: The insolation canon hypothesis. *Earth and Planetary Science Letters*, *249*, 326–336. https://doi.org/10.1016/j.epsl.2006.07.004

Seki, O., Foster, G. L., Schmidt, D. N., Mackensen, A., Kawamure, K., & Pancost, R. D. (2010). Alkenone and boron-based Pliocene pCO_2 records. *Earth and Planetary Science Letters*, *292*, 201–211. https://doi.org/10.1016/j.epsl.2010.01.037

Sellers, W. D. (1969). A global climatic model based on the energy balance of the Earth-atmosphere system. *Journal of Applied Meteorology*, *8*, 392–400. https://doi.org/10.1175/1520-0450(1969)008<0392:agcmbo>2.0.co;2

Shackleton, N. J., & Opdyke, N. D. (1976). Oxygen-isotope and paleomagnetic stratigraphy of Pacific Core V28-239 Late Pliocene to Latest Pleistocene (Vol. 145, pp. 449–464). In Geological Society of America Memoir. https://doi.org/10.1130/mem145-p449

Snyder, C. W. (2016). Evolution of global temperature over the past two million years. *Nature*, *536*, 226–228. https://doi.org/10.1038/nature19798

Sosdian, S. M., Greenop, R., Hain, M. P., Foster, G. L., Pearson, P. N., & Lear, C. H. (2018). Constraining the evolution of Neogene ocean carbonate chemistry using the boron isotope pH proxy. *Earth and Planetary Science Letters*, *498*, 362–376. https://doi.org/10.1016/j.epsl.2018.06.017

Stap, L. B., de Boer, B., Ziegler, M., Bintanja, R., Lourens, L. J., & van de Wal, R. (2016). CO_2 over the past 5 million years: Continuous simulation and new d11B-based proxy data. *Earth and Planetary Science Letters*, *439*, 1–10. https://doi.org/10.1016/j.epsl.2016.01.022

Stap, L. B., van de Wal, R. S. W., de Boer, B., Köhler, P., Hoencamp, J. H., Lohmann, G., et al. (2018). Modeled influence of land ice and CO_2 on polar amplification and paleoclimate sensitivity during the past 5 million years. *Paleoceanography and Paleoclimatology*, *33*, 381–394. https://doi.org/10.1002/2017pa003313

Stults, D. Z., Wagner-Cremer, F., & Axsmith, B. J. (2011). Atmospheric paleo-CO_2 estimates based on Taxodium distichum (Cupressaceae) fossils from the Miocene and Pliocene of Eastern North America. *Palaeogeography, Palaeoclimatology, Palaeoecology*, *309*, 327–332. https://doi.org/10.1016/j.palaeo.2011.06.017

Sutter, J., Fischer, H., Grosfeld, K., Karlsson, N. B., Kleiner, T., Van Liefferinge, B., & Eisen, O. (2019). Modeling the Antarctic Ice Sheet across the Mid-Pleistocene transition – implications for Oldest Ice. *The Cryosphere*, *13*, 2023–2041. https://doi.org/10.5194/tc-13-2023-2019

Tzedakis, P. C., Crucifix, M., Mitsui, T., & Wolff, E. W. (2017). A simple rule to determine which insolation cycles lead to interglacials. *Nature*, *542*, 427–432. https://doi.org/10.1038/nature21364

Tziperman, E., Raymo, M. E., Huybers, P., & Wunsch, C. (2006). Consequences of pacing the Pleistocene 100 kyr ice ages by nonlinear phase locking to Milankovitch forcing. *Paleoceanography*, *21*. https://doi.org/10.1029/2005pa001241

van de Berg, J., van de Wal, R. S. W., & Oerlemans, J. (2008). A mass balance model for the Eurasian Ice Sheet for the last 120,000 years. *Global and Planetary Change*, *61*, 194–208. https://doi.org/10.1016/j.gloplacha.2007.08.015

van de Wal, R. S. W., de Boer, B., Lourens, L. J., Köhler, P., & Bintanja, R. (2011). Reconstruction of a continuous high-resolution CO_2 record over the past 20 million years. *Climate of the Past*, *7*, 1459–1469. https://doi.org/10.5194/cp-7-1459-2011

Veres, D., Bazin, L., Toyé Mahamadou Kele, H., Lemieux-Dudon, B., Parrenin, F., Martinerie, P., et al. (2013). The Antarctic ice core chronology (AICC2012): An optimized multi-parameter and multi-site dating approach for the last 120 thousand years. *Climate of the Past*, *9*, 1733–1748. https://doi.org/10.5194/cp-9-1733-2013

Wang, P., Tian, J., & Lourens, L. J. (2010). Obscuring of long eccentricity cyclicity in Pleistocene oceanic carbon isotope records. *Earth and Planetary Science Letters*, *290*, 319–330. https://doi.org/10.1016/j.epsl.2009.12.028

Weertman, J. (1961). Stability of Ice-Age Ice Sheets. *Journal of Geophysical Research*, *66*, 3783–3792. https://doi.org/10.1029/jz066i011p03783

Werner, M., Jouzel, J., Masson-Delmotte, V., & Lohmann, G. (2018). Reconciling glacial Antarctic water stable isotopes with ice sheet topography and the isotopic paleothermometer. *Nature Communications*, *9*. https://doi.org/10.1038/s41467-018-05430-y

Willeit, M., Ganopolski, A., Calov, R., & Brovkin, V. (2019). Mid-Pleistocene transition in glacial cycles explained by declining CO and regolith removal. *Science Advances*, *5*. https://doi.org/10.1126/sciadv.aav7337

Williams, D. F., Thunell, R. C., Tappa, E., Rio, D., & Raffi, I. (1988). Chronology of the Pleistocene oxygen isotope record: 0-1.88 m.y. B.P. *Palaeogeography, Palaeoclimatology, Palaeoecology*, *64*, 221–240. https://doi.org/10.1016/0031-0182(88)90008-9

Wunsch, C. (2003). The spectral description of climate change including the 100 ky energy. *Climate Dynamics*, *20*, 353–363. https://doi.org/10.1007/s00382-002-0279-z

Yan, Y., Bender, M. L., Brook, E. J., Clifford, H. M., Kemeny, P. C., Kurbatov, A. V., et al. (2019). Two-million-year-old snapshots of atmospheric gases from Antarctic ice. *Nature*, *574*, 663–666. https://doi.org/10.1038/s41586-019-1692-3

Zhang, Y. G., Pagani, M., Liu, Z., Bohaty, S. M., & DeConto, R. M. (2013). A 40-million year history of atmospheric CO_2. *Philosophical Transactions of the Royal Society A*, *371*. https://doi.org/10.1098/rsta.2013.0096